Refractometry models for compositional analysis of binary and ternary mixtures

Franco Pretorius

Refractometry models for compositional analysis of binary and ternary mixtures

by

Franco Pretorius

Submitted in fulfilment of the requirements for the degree

Master of Engineering (Chemical Engineering)

in the

Department of Chemical Engineering

University of Pretoria

Supervisor: Prof. WW Focke

Co-supervisor: Ms EL du Toit

2024

Refractometry models for compositional analysis of binary and ternary mixtures

Abstract

A review of existing compositional binary mixture models for refractive indices was undertaken and showed that they can be recast in forms that are linear in mole or volume fraction. Typically, mole fractions proved to be the better composition descriptor when analysing literature data and the molar refraction was shown to be virtually temperature independent. Depending on whether temperature, density or refractive index measurements of the mixture are available, different correlations were developed to predict the composition (as shown below). Furthermore, refractive index measurements on mixtures of *n*-alkanes with DEET were taken to determine phase equilibrium behaviour. With extrapolation to infinite molar mass, these alkanes approach polyethylene, which is the material from which DEET-containing mosquito-repellent devices were made. The results show that the microporous structure was likely formed by liquid-liquid phase separation. Lastly, it was shown that Padé approximants provide good representations of binary and ternary refractive index data. The temperature dependence of the pure components was elegantly subsumed in a pure component property, namely, the molar volume. Various constraints were applied to reduce the number of adjustable parameters even further and this proved to be successful.

Keywords: refractive index, polymer solutions, phase equilibrium, *n*-alkanes

Definitions

Single components

$$N_i = \frac{n_i^2 - 1}{n_i^2 + 2} \qquad V_i = \frac{M_i}{\rho_i} \qquad R_i = V_i N_i \qquad w_i = \frac{M_i x_i}{\sum_m M_i x_i} \qquad \varphi_i = \frac{V_i x_i}{\sum_m V_i x_i}$$

Mixtures

$$N = \frac{n_{mix}^2 - 1}{n_{mix}^2 + 2} \qquad V = \frac{M}{\rho} \qquad M = \Sigma_m M_i x_i \qquad x_1 + x_2 = 1 \qquad \varphi_1 + \varphi_2 = 1$$

(binary mixture)

Measured inputs

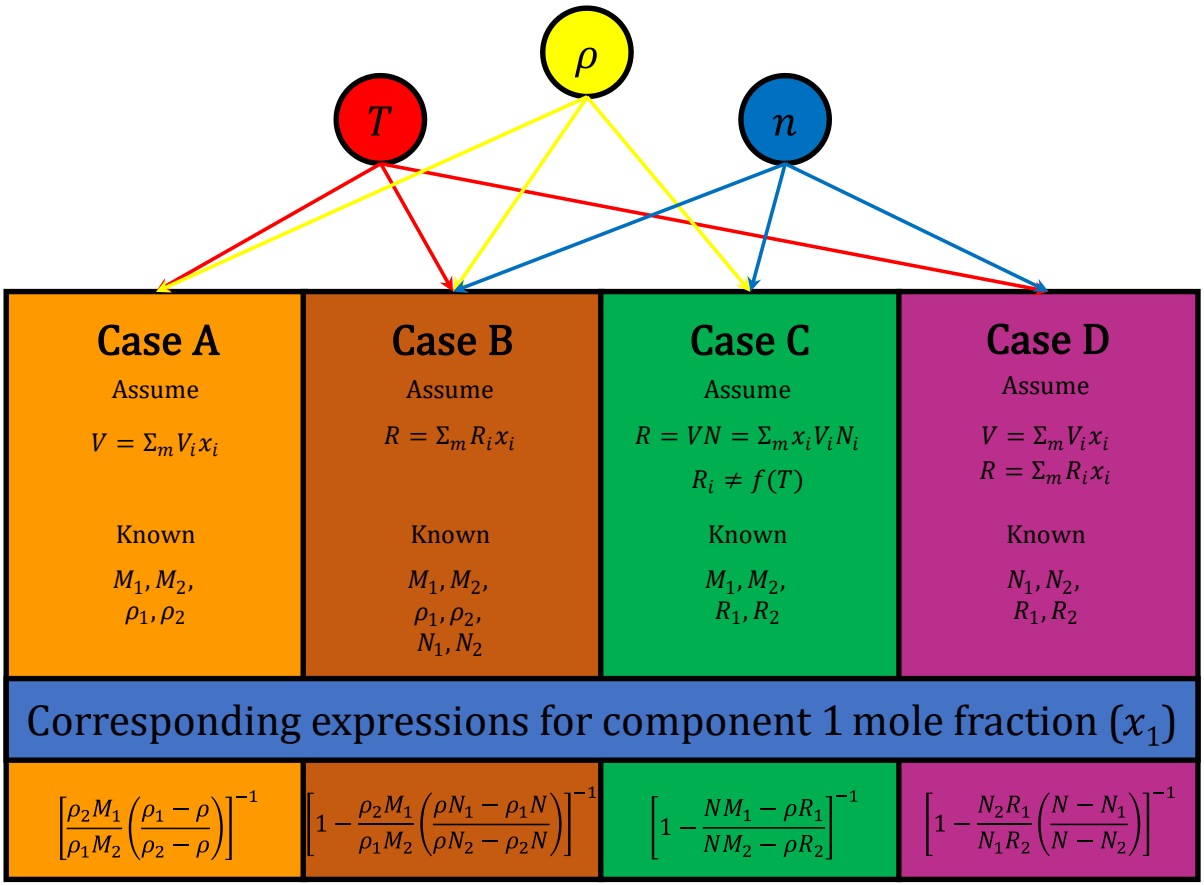

Acknowledgements

I am indebted to so many for their support during this project:

- Firstly, to God who gave me the strength and wisdom to undertake this project.
- Prof. Walter Focke and Ms. Elizbé du Toit for their guidance and mentorship during this project. Thank you for major assistance with analysis, feedback on my work and for truly impacting me and shaping the start of my professional development.
- Pethile Dzingai and Kgaugelo Mashiachidi for assistance in gathering literature data.
- Dr Isbé van der Westhuizen for her plentiful assistance in the laboratory.
- CSIR for generous bursary support.
- Lastly, my parents, family members and friends for your love, help, patience, and prayers.

I really appreciate you all!

All the darkness in the world cannot extinguish the light of a single candle.

—St. Francis Of Assisi

Your word is a lamp for my feet, a light on my path.

—Psalms 119:105

It's better to light a single candle than to curse the darkness.

—English proverb

Declaration

I hereby declare that this manuscript is my own original work and has not previously been submitted to any other institution of higher education. Furthermore, all sources cited or quoted are indicated and acknowledged by means of a comprehensive list of references. Extensive portions of this work have already been published and are indicated as such in the text.

Franco Pretorius	2024-01-23
Signatory name	Date

Contents

List of figures

List of tables

Nomenclature

A	Interaction parameter constant	
A	System-dependent critical amplitudes	
a	Sphere radius	m
AAD	Average absolute deviations	%
AIC	Akaike information criterion	
ΔAIC	Difference in Akaike information criterion	
B	Bernstein polynomial	
B	Interaction parameter constant	
B	System-dependent critical amplitudes	
b	Bernstein basis polynomial	
c	Speed of light in a vacuum (299 792 458)	$m \cdot s^{-1}$
d	Diameter of coexistence curve	
d	Modified Eykman parameter	
df	Degrees of freedom	
G	Gibbs free energy	J
M	Molar mass	$kg \cdot mol^{-1}$
m	Adjustable constant for the phase envelope	
m	Mass	kg
m	Total number of components	
N	Lorentz-Lorenz parameter of refractive index	-
N_A	Avogadro's number ($6.022\ 140\ 76 \times 10^{23}$)	mol^{-1}
n	Mole	mol
n	Number of data points	
n	Polynomial degree	
n	Refractive index	
P	Padé approximant	
P	Polynomial	
P	Pressure	Pa
p	Physical property	
p	Order of weighted power mean parameter	
q	General composition variable (q-fraction)	

R_g	Universal gas constant (8.314)	$J \cdot mol^{-1} \cdot K^{-1}$
R	Molar refraction	$m^3 \cdot mol^{-1}$
r	Correlation coefficient	
r	Modified refractive index variable	
s	Standard deviation	
SSE	Sum of the square errors	
T	Temperature	K
V	Molar volume	$m^3 \cdot mol^{-1}$
v	Volume	m^3
w	Mass fraction	-
X	Ratio of polymer to solvent molar volume	
x	Mole fraction	-
z	Composition variable	
Greek		
α	Angle of light relative to normal line	°
α	Critical exponent	
α	Mean molecular polarizability of nonpolar, nonmagnetic materials	$F \cdot m^2$
β	Adjustable constant	
β	Angle of refraction	°
β	Pure component property	
β	Universal critical exponent (0.326)	
Δ	Universal critical exponent (0.50)	
δ	Kronecker delta	
ε_0	Vacuum permittivity ($8.8541878128 \times 10^{-12}$)	$F \cdot m^{-1}$
θ	Adjustable constant	
κ	Adjustable constant	
λ	Adjustable constant	
ν	Speed of light in a medium	$m \cdot s^{-1}$
ρ	Density	$kg \cdot m^{-3}$
τ	Adjustable constant	
τ	Reduced temperature	

υ	Specific volume	$m^3 \cdot kg^{-1}$
φ	Volume fraction	-
χ	Flory-Huggins interaction parameter	
ω	Adjustable constant	

Subscripts

1, 2	Component 1, component 2
c	Critical
i	Component *i*
i	Internal
k	Index of term
L	Left branch of coexistence curve
mix	Mixture
n	Polynomial of degree *n*
R	Right branch of coexistence curve
r	Reflection

Abbreviations

DEET	*N*,*N*-diethyl-*meta*-toluamide
L-L-N	Lorentz-Lorenz *N*-mixing rule
L-L-R	Lorentz-Lorenz *R*-mixing rule
PLLA	Poly(L-lactic acid)
RI	Refractive index
TIPS	Temperature induced phase separation
UCST	Upper critical solution temperature

1 Introduction

Recent research efforts in the Institute of Applied Materials have focused on malaria vector control. This included the invention of socks (made in part with bicomponent fibres) (Sibanda *et al*, 2018), bracelets, anklets (Mapossa *et al*, 2019), and strands (Sitoe *et al*, 2020) for the controlled release of mosquito repellents. The latter research effort entailed creating microporous polyethylene strands containing *N*,*N*-diethyl-*meta*-toluamide (DEET) by temperature induced phase separation (TIPS) known as spinodal decomposition. The question arose as to whether this was accomplished via liquid-liquid phase separation or by crystallisation-induced solid-liquid phase separation, the latter of which was the case for the poly(lactic acid) (PLLA)-DEET system (Sungkapreecha *et al*, 2020). Initial attempts were made to determine the phase boundary by differential scanning calorimetry (DSC) of mixtures of DEET and *n*-alkanes of increasing chain length (which extrapolates towards polyethylene at infinite molar mass). However, this proved to be unsuccessful due to the negligible enthalpy of demixing (Sitoe *et al*, 2021).

Therefore, it was decided to explore the use of refractometry for this analysis. It is known that the refractive index of a pure component or mixture of fixed composition varies linearly with temperature (Riazi *et al*, 1999). Therefore, when scanning the temperature, a sudden deviation from the linear trend could indicate a change in composition at that temperature, i.e., that phase separation occurred (Sitoe *et al*, 2021). This study then originated as supporting work for understanding how to correlate physical property data, specifically refractive index, with temperature and composition.

Firstly, a review was conducted on binary theoretical and empirical models which are used to express refractive index as a function of composition. Secondly, this concept was applied to establish the approximate phase boundaries for a homogenous series of DEET and alkane mixtures. This is because the melting temperature of polyethylene was far above the maximum temperature which the refractometer could reach (viz., 100 °C). A novel technique was then applied to fit the phase boundary data near the critical temperature through enabling asymmetry of the coexistence curve (Damay and Leclercq, 1991). By extrapolation, the likely behaviour of polyethylene was estimated (Sitoe *et al*, 2021).

When this investigation was completed, another student in the research group, namely Pethile Dzingae, needed assistance with examining models for expressing surface tension as a function of composition and temperature. In assisting with resolving this issue, it was found that most of the theoretical and empirical models for the surface tension of binary mixtures could be recast in the form of Padé approximants. Excellent data fits were achieved with these models (Dzingai *et al*, 2024). This posed the question whether a similar approach could work for the refractive index. This proved to be the case. It was found that literature data for the refractive index of ternary systems, measured over certain temperature ranges could be fitted with a single expression using Padé approximants of order (2, 2) (Pretorius *et al*, 2024).

In summary, this dissertation traces a journey that started out as a comprehensive literature survey on the mixture models for the refractive index of binary mixtures, the application of one of those models to the establishment of liquid-liquid phase diagrams for alkane-DEET mixtures and, ultimately, culminating in the development of novel mixture models suitable for correlating multicomponent data over a range of temperatures.

2 Literature

2.1 Liquid mixture properties

In order to correlate any physical property of a liquid mixture, it is necessary to define the mixture composition. A mixture is a "portion of matter consisting of two or more chemical substances called constituents" (IUPAC, 2006) which are not chemically bonded. A homogenous mixture is a mixture of a single phase with uniform composition.

Several composition variables are typically used to describe the ratio of one compound to the total number of compounds (m) in the mixture. When expressed as fractions, they must sum to unity. This is known as the simplex constraint.

Firstly, on a mass basis, the mass fraction is defined as the mass of component i relative to the total mass of the mixture, m_{mix}

$$w_i \equiv \frac{m_i}{m_{mix}} = \frac{m_i}{\sum_{i=1}^{m} m_i} \tag{1}$$

Secondly, when the mass of a component is divided by its molar mass, M_i, the mole amount of component i, n_i is obtained. Similar to the mass fraction, the mole fraction is defined relative to the total number of moles in the mixture

$$x_i \equiv \frac{n_i}{n_{mix}} \tag{2}$$

The mass fraction can also be calculated from the mole fractions as

$$w_i = \frac{M_i x_i}{\sum_{i=1}^{m} M_i x_i} \tag{3}$$

Thirdly, the volume of a component, v_i, relative to the total volume of the mixture, v_{mix}, can be used to define the volume fraction

$$\varphi_i \equiv \frac{v_i}{v_{mix}} \tag{4}$$

The volume fraction can also be calculated from the mole fractions and molar volumes as

$$\varphi_i = \frac{V_i x_i}{\sum_{i=1}^{m} V_i x_i} \tag{5}$$

The volume fraction is challenging to apply in practise as many mixtures exhibit nonideal mixing. In other words, the true sum of the constituent volumes does not equate to the measured mixture volume.

Wohl (1946) defined a general composition variable in terms of *q*-fractions as

$$q_i = \frac{\beta_i x_i}{\sum_{i=1}^{m} \beta_i x_i} \tag{6}$$

Here, the β_i coefficients are a suitable pure component property. For instance, if $\beta_i = M_i$ the q-fraction becomes the mass fraction as per Equation (3). If $\beta_i = V_i$, the q-fraction becomes the volume fraction as per Equation (5). If these coefficients are just treated as adjustable parameters, they cannot be determined uniquely, because they can be multiplied by any constant without affecting the value of the q-fraction. This problem can be overcome by imposing a restriction on the value of one of the β_i values or by restricting their sum to unity.

In addition to composition, mixture properties are functions of temperature and pressure. For many liquid properties, temperature is important, but the pressure dependence is often quite weak so that it can be neglected. This is especially the case for refractive index of liquid mixtures, which has found extensive use for compositional analysis.

2.2 Refractometry

Refractive index (RI) measurements are commonly used for liquid mixture composition analysis (Martens *et al*, 2020). For example, this includes sugar, salt and alcohol content determination (Shehadeh *et al*, 2020). This technique operates by the principle of refraction.

The index of refraction, *n*, is given by

$$n = \frac{c}{v} \tag{7}$$

where *c* is the speed of light, and *v* is the speed of light in a material (Gallegos and Stokkermans, 2023). Temperature also affects the refractive index as increasing the temperature usually leads

to decreased density of the substrate. The resultant refractive index decreases because light travels faster in a less dense medium (Waxler and Cleek, 1973).

A light beam incident on the interface between two media of different optical density will refract, i.e., change its direction, as shown in Figure 1. Depending on the angle of incidence, α_i, this results in splitting of the beam in a refracted portion, i.e., the part that proceeds in another medium, and in a reflected portion. Total internal reflection only takes place when two conditions are met, namely, that the light is in the denser medium and approaching the less dense medium, and that the angle of incidence is greater than the critical angle α_c. The critical angle is specific to a boundary system, i.e., the refractive indices of the two media.

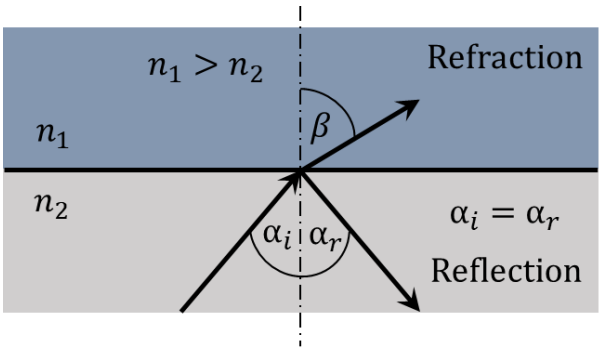

Figure 1: Reflection and refraction of light (Korotchenkov, 2011: 317).

At α_c the angle of refraction (β) is 90°. Refraction is described by Snell's law (Korotchenkov, 2011: 317):

$$n_1 \sin \alpha_i = n_2 \sin \beta \tag{8}$$

where n_1 describes the refractive index of the optically denser medium and n_2 is the refractive index of the optically less dense medium. Note that light is bent away from the normal when traveling into a material with a lower refractive index. The refraction angle is measured by instruments known as refractometers.

Modern refractometers are digital and use an LED to illuminate a sample placed on the prism, typically with the spectral D-lines of sodium, n_D = 589.3 nm (Wypych, 2017). The refracted light is then measured with a sensor that determines the refraction angle, and the temperature is also recorded (Rodrigues, 2023). This value is then converted by algorithms into a refractive index. Benchtop refractometers are more accurate compared to analogue and digital refractometers; however, they are more expensive (Jaywant *et al*, 2022).

The history of the first refractometer is difficult to determine. Ernst Abbé developed his first refractometer in 1869 for Carl Zeiss in order to produce optical glass. Its first use beyond this was by Harvey Wiley in 1888 to distinguish butter from a beef-based alternative oleomargarine. Zeiss noted in 1893 that refractometers could be used "to distinguish many substances and to ascertain their degree of purity (adulteration of victuals), or to determine the percentage or concentration of many solutions and mixtures" (Warner, 2010). It has since found applications in the analysis of fats, oils, waxes, sugars, syrups, essential oils, glue, gelatine, petroleum, paint, varnish, gas, alcohol, and drugs (Warner, 2010).

In order to analyse the composition of a mixture, a calibration curve for refractive index (n) *vs.* composition should be available and should be a monotonic function of mole fraction or mass fraction of one of the components. Such a calibration curve would usually only be available at a fixed temperature.

Many different functions for the compositional variance in binary liquid mixtures have been developed over the years.

2.3 Mixing rules for the refractive index

This Section reflects work presented in the first article dealing with the subject at hand (Pretorius *et al*, 2021).

2.3.1 Pure components

The molar refraction (R) for nonpolar, nonmagnetic materials is defined (Prausnitz *et al*, 1999) as

$$R = \alpha N_A/(3\varepsilon_o) \tag{9}$$

where α is the mean molecular polarisability; N_A is Avogadro's number; and ε_o is the permittivity of free space. For a fluid of hard-core spheres of uniform size, the polarisability is given by

$$\alpha = 4\pi\varepsilon_o a^3 \tag{10}$$

where a represents the sphere radius. Substitution of Equation (10) into Equation (9) results in

$$R = \frac{4\pi}{3} N_A a^3 \tag{11}$$

For such a hypothetical fluid, the molar refraction can be interpreted as the hard core volume of one mole of spherical molecules of radius *a* (Prausnitz *et al*, 1999). These expressions have found applications for real organic liquids and their mixtures despite their simple, theoretical origins.

A much more prevalent model is the Lorentz–Lorenz relationship. It was established independently, first in 1869 by L. V. Lorenz (in the field of optics) and subsequently in 1878 by H. A. Lorentz (from electromagnetism) (Kragh, 2018). This equation links the molar refraction with the refractive index and the molar volume (Heller, 1965):

$$R = V\frac{n^2-1}{n^2+2} \tag{12}$$

where the molar volume V is defined by the ratio of the molar mass (M) to the density (ρ) of the compound

$$V = \frac{M}{\rho} \tag{13}$$

Experimental evidence indicates that the molar refraction of a pure compound is approximately temperature invariant (Vargas and Chapman, 2010). Furthermore, for hydrocarbons, including alkanes, the so-called “one third rule” applies which states (Vargas and Chapman, 2010):

$$\frac{R}{M} = \frac{1}{\rho}\left(\frac{n^2-1}{n^2+2}\right) \approx \frac{1}{3} \tag{14}$$

2.3.2 Binary mixtures

An ideal binary solution would follow the linear blending rule for molar volume (Brocos *et al*, 2003):

$$V = V_1x_1 + V_2x_2 \tag{15}$$

When the mixture density data are known, the molar volume behaves as for an ideal solution, and since x_1+x_2 = 1, Equation (15) and Equation (13) allow the composition to be calculated from

$$\frac{1}{x_1} = 1 - \frac{\rho_2 M_1(\rho_1-\rho)}{\rho_1 M_2(\rho_2-\rho)} \tag{16}$$

See Appendix A.1 Case A for the derivation of Equation (16). Theoretical considerations (Brocos *et al*, 2003) suggest that the molar refraction of an ideal binary liquid mixture is also additive on a mole fraction basis

$$R = R_1 x_1 + R_2 x_2 \tag{17}$$

Substitution of R from Equation (12) in Equation (17) yields the Lorentz-Lorenz R-mixing (*L-L-R*) rule

$$V \frac{n_{mix}^2 - 1}{n_{mix}^2 + 2} = V_1 x_1 \frac{n_1^2 - 1}{n_1^2 + 2} + V_2 x_2 \frac{n_2^2 - 1}{n_2^2 + 2} \tag{18a}$$

or, expressed in a more general form:

$$R = VN = x_1 V_1 N_1 + x_2 V_2 N_2 \tag{18b}$$

where the following definitions were applied

$$N = \left(n_{mix}^2 - 1\right) \Big/ \left(n_{mix}^2 + 2\right) \text{ and } N_i = \left(n_i^2 - 1\right) \Big/ \left(n_i^2 + 2\right) \tag{19}$$

The calculation of the molar refraction R of a mixture requires information about the density and the refractive index. When both are available, the composition of the mixture can be established directly in terms of the mole fraction of component 1

$$\frac{1}{x_1} = 1 - \frac{\rho_2 M_1 \left(\rho N_1 - \rho_1 N\right)}{\rho_1 M_2 \left(\rho N_2 - \rho_2 N\right)} \tag{20}$$

See Appendix A.1 Case B for the derivation of Equation (20). Density data for the pure components, at the mixture temperature, are required when applying Equation (20). However, this is not essential. If the molar refractions R_1 and R_2 are known and if they are temperature-invariant, then $R_i = M_i N_i / \rho_i$. Thus, the composition can also be estimated with a different expression

$$\frac{1}{x_1} = 1 - \frac{NM_1 - \rho R_1}{NM_2 - \rho R_2} \tag{21}$$

See Appendix A.1 Case C for the derivation of Equation (21). Its application allows direct calculation of the component mole fractions from simultaneous measurements of just the density and the refractive index of the mixture. In other words, it is not necessary to know the temperature.

When there is no information available for the mixture density, another approach must be followed. The required relationship is labelled the Lorentz-Lorenz *N*-mixing rule (*L-L-N*) which is established by combining Equation (15) and Equation (18). This gives

$$\frac{n_{mix}^2-1}{n_{mix}^2+2}=\varphi_1\frac{n_1^2-1}{n_1^2+2}+\varphi_2\frac{n_2^2-1}{n_2^2+2} \tag{22a}$$

or

$$N=\varphi_1 N_1+\varphi_2 N_2 \tag{22b}$$

where the volume fraction, at the mixture temperature, is defined in terms of the pure component molar volumes (V_i) as follows

$$\varphi_i \equiv V_i x_i/(V_1 x_1+V_2 x_2) \tag{23}$$

Numerous studies found that, for many real mixtures, predictions of mixture refractive indices according to the modified Lorentz-Lorenz relationship, i.e. the *L-L-N* mixing rule of Equation (22), agree reasonably well with experimental results (Heller, 1965; Iglesias-Otero *et al*, 2008; Krishnaswamy and Janzen, 2005; Tasic *et al*, 1992). Equation (22) allows direct estimation of the volume fraction of an equilibrium phase from refractive index measurements, expressed in terms of *N*-values as follows

$$\varphi_1=(N-N_2)/(N_1-N_2) \tag{24}$$

The n_i values must be known at the mixture temperature in order to calculate the N_i. The mole fraction and mass fraction can then be established from the following relationships

$$\frac{1}{x_1}=1-\frac{N_2R_1(N-N_1)}{N_1R_2(N-N_2)} \tag{25}$$

and (from Equation (3))

$$w_1=M_1x_1/(M_1x_1+M_2x_2) \tag{26}$$

See Appendix A.1 Case D for the derivation of Equation (25). Equation (25) shows that the mole fraction of component 1 can be calculated directly using the measured value for the refractive index of the mixture. However, knowledge of the pure component values at the system temperature are required.

It is important to note the basic assumptions that underlie the key expressions developed for estimating the composition of binary mixtures. Equation (20), Equation (21) and Equation (25)

assume that the molar refraction corresponds to the expectations for an ideal solution as expressed by Equation (17). Use of Equation (20) also requires knowledge of the mixture and component densities in addition to refractive index data. In contrast, Equation (25) does not require density data for the mixture for its application. However, it relies on an additional assumption, i.e., that the molar volume follows the expression applicable to an ideal solution as stated in Equation (15). Furthermore, if both properties conform to the expectations for an ideal solution, it can be shown by combining Equations (13), (15), and (18b) that the following expression holds

$$N = \frac{\rho_2 M_1 N_1 x_1 + \rho_1 M_2 N_2 x_2}{\rho_2 M_1 x_1 + \rho_1 M_2 x_2} \tag{27}$$

Equation (27) represents the simplest mixing rule for ideal solutions. It indicates that the mixture refractive index is fully defined by knowledge of the densities, molar masses, and refractive indices of the pure components.

Table 1 summarises the relationships derived for four different measurement cases. Note that, in some cases, it is assumed that the system temperature is also known and that correlations exist for calculating the required pure component properties.

Table 1: Different measurement combinations for temperature (T), density (ρ) and refractive index (n)

Case	T	ρ	n	Assumptions	Known	Measured	Expression for x_1
A	✓	✓		$V = V_1x_1+V_2x_2$	M_1, M_2, ρ_1, ρ_2	ρ	$\left[1-\frac{\rho_2 M_1}{\rho_1 M_2}\left(\frac{\rho_1-\rho}{\rho_2-\rho}\right)\right]^{-1}$
B	✓	✓	✓	$R = R_1x_1+R_2x_2$	M_1, M_2, ρ_1, ρ_2, n_1, n_2	ρ, n	$\left[1-\frac{\rho_2 M_1(\rho N_1-\rho_1 N)}{\rho_1 M_2(\rho N_2-\rho_2 N)}\right]^{-1}$
C		✓	✓	$R = R_1x_1+R_2x_2$ $R_i \neq f(T)$	M_1, M_2, R_1, R_2	ρ, n	$\left[1-\frac{NM_1-\rho R_1}{NM_2-\rho R_2}\right]^{-1}$
D	✓		✓	$V = V_1x_1+V_2x_2$ $R = R_1x_1+R_2x_2$	R_1, R_2, n_1, n_2	n	$\left[1-\frac{N_2 R_1(N-N_1)}{N_1 R_2(N-N_2)}\right]^{-1}$

2.3.3 Alternative mixing rules

Numerous other mixing rules have been proposed with the hope to improve the Lorentz-Lorenz approach detailed above. Eyring and John (1969) and Lichtenecker (Heller, 1945) proposed nonlinear mixing rules for the refractive index (n). However, as shown below, their proposals can be recast in linear forms.

Eyring and John (1969):

$$n = \left(\varphi_1\sqrt{n_1} + \varphi_2\sqrt{n_2}\right)^2 \tag{28a}$$

$$\sqrt{n} = \varphi_1\sqrt{n_1} + \varphi_2\sqrt{n_2} \tag{28b}$$

Lichtenecker:

$$n = n_1^{\varphi_1} n_2^{\varphi_2} \tag{29a}$$

$$\ln n = \varphi_1 \ln n_1 + \varphi_2 \ln n_2 \tag{29b}$$

This means that most proposals introduced changes to the expression used for N but retained the linear composition dependence on the volume fraction as defined by Equation (22b). Comparison of the linear forms of the Eyring and John (1969) and Lichtenecker, as well as numerous other mixture rule proposals, reveals that they correspond to the same family of volume-fraction-weighted power means of order p defined by

$$n_p = \left(\varphi_1 n_1^p + \varphi_2 n_2^p\right)^{1/p} \tag{30}$$

This expression includes the geometric mixing rule defined by Lichtenecker, as it corresponds to the limiting case where the power index approaches zero from above ($p \to 0^+$).

Table 2 summarises the mixing rules reported in the literature for the refractive index of binary mixtures. More complex models include the proposals by Heller (1945) and Wiener (1910). The Heller model is limited to low concentrations of the dispersed phase, i.e. φ_2, while the Wiener (1910) equation is valid over the full composition range. It can be shown that Wiener's proposal is equivalent to the following Padé-type mixing rule (see Section 2.5)

$$n^2 = \frac{n_1^4\varphi_1 + 2n_1^2 n_2^2 + n_2^4\varphi_2}{n_1^2\left(2-\varphi_1\right) + n_2^2\left(2-\varphi_2\right)} \tag{31}$$

Several studies compared the relative performance of some of the mixture models listed in Table 2 (Pandey *et al*, 2007; Sirbu *et al*, 2019; Tasic *et al*, 1992; Vuksanović *et al*, 2014). It was mentioned that the Arago–Biot mixing rule offered the worst experimental data fit (Radović *et al*, 2008; Vuksanović *et al*, 2014). Most studies concluded that the Lorentz-Lorenz relations gave the best correlation for all systems investigated (Heller, 1965; Iglesias-Otero *et al*, 2008; Krishnaswamy and Janzen, 2005; Mehra, 2003; Tasic *et al*, 1992). However, no-one considered the Looyenga (1965) model.

Table 2: Summary of the mixing rules proposed in the literature including possible definitions for the variable N in Equation (18b) or in Equation (22b)

Model type	Model	Expression	Reference
$VN = V_1N_1x_1 + V_2N_2x_2$ with $N = (n^2 - 1)/(n^2 + d)$	Lorentz-Lorenz	$d = 2$	(Eykman and Holleman, 1919; Piñeiro *et al*, 1999)
	Eykman	$d = 0.4$	
	Modified Eykman	variable d	
$VN = V_1N_1x_1 + V_2N_2x_2$ with revised expressions for N	Oster	$N = (n^2-1)(2n^2+1)/n^2$	(Oster, 1948)
	Looyenga	$N = n^{2/3} - 1$	(Looyenga, 1965)
	Arago-Biot	$N = n$	(Arago and Biot, 1806)
	Dale-Gladstone	$N = n - 1$	(Dale and Gladstone, 1858)
	Newton	$N = n^2 - 1$	(Kurtz and Ward, 1936)
Volume fraction weighted power mean of order p: $n = \left(\varphi_1 n_1^p + \varphi_2 n_2^p\right)^{1/p}$	Lichtenecker	$p = 0$	(Heller, 1945)
	Eyring	$p = 1/2$	(Eyring and John, 1969)
	Looyenga	$p = 2/3$	(Looyenga, 1965)
	Arago-Biot & Dale-Glastone	$p = 1$	(Arago and Biot, 1806; Dale and Gladstone, 1858)
	Newton	$p = 2$	(Kurtz and Ward, 1936)
		p variable	This work
Complex models	Heller (valid for low values of φ_2)	$\varphi_2 = \frac{2\left(n-n_1\right)\left[n_2^2+2n_1^2\right]}{3n_1\left(n_2^2-n_1^2\right)}$	(Heller, 1945)
	Wiener	$\varphi_2 = \left(\frac{n^2-n_1^2}{n_2^2-n_1^2}\right)\left(\frac{n_2^2+2n_1^2}{n^2+2n_1^2}\right)$	(Heller, 1945) (Wiener, 1910)

2.4 Polymer-solution phase equilibrium

Polymer solutions are mixtures which consist of a polymer (a component with long macromolecular chains), and a solvent (small molecules) (Grosberg *et al*, 1998). This mixture may exist as a liquid or as a solid. These mixtures are used to manufacture composites such as fibres, films, glues, paints, light-emitting devices (Chang *et al*, 1999), and, as mentioned previously, long-life personal protective wear against mosquitoes. The manufacturing process for microporous structures relies on temperature induced phase separation (TIPS) (Castro, 1981; Lloyd *et al*, 1990; Ulbricht, 2006) to create a microporous polymer structure that traps a large quantity of the liquid repellent (Mapossa *et al*, 2020). Firstly, a fully homogeneous solution of the repellent in the polymer melt is created above the upper critical solution temperature (UCST). Phase separation is then induced by rapidly cooling it into the spinodal region. This means that the polymer processing temperature should exceed the UCST before the forced rapid cooling step commences.

If a crystallisable polymer is present, it is not always clear whether the phase separation initiates via liquid-liquid phase separation or via polymer crystallisation. These mechanisms differ with respect to both the transformation kinetics and the resulting microstructure which ultimately controls the repellent release characteristics. Specifically, the DEET-polyethylene system is considered here.

Thermodynamic models have been used to model polymer solutions. In the most basic sense, ideal solutions can be considered as lattices of molecules that are firstly identical in size, and secondly, exhibit equal energies for like and unlike molecular interactions (Young and Lovell, 2011: 238). However, both of these assumptions are untrue in the case of polymer-solvent systems.

2.4.1 Flory-Huggins theory

Flory (1941) and Huggins (1941) independently derived a modified lattice theory which is still commonly used today. The Flory-Huggins solution theory is based on the following simplifying assumptions (Danner and High, 1993):

- No change in volume upon mixing (i.e., it is a strict lattice model with ideal chains)
- The composition of each polymer is not treated individually
- The interaction parameter is independent of composition

- The only contribution to possible states is translational configurations
- Molecules of a given type are indistinguishable and mix randomly

Akhtar and Focke (2015) established the coexistence curves for the citronellal-polyethylene system using hot-stage microscopy in the cooling mode. However, difficulties were experienced with such measurements of the cloud points for mixtures of polyethylene with the mosquito repellent DEET. Therefore, the Flory-Huggins theory was applied. Assuming that each solvent molecule and polymer segment occupy exactly one lattice site, one obtains (Young and Lovell, 2011: 244):

$$\frac{\Delta G_{mix}}{R_g T} = \chi \varphi_1 \varphi_2 + \varphi_1 \ln \varphi_1 + \left(\frac{\varphi_2}{X} \right) \ln \varphi_2 \tag{32}$$

where ΔG_{mix} is the molar Gibbs free energy of mixing per mole of lattice sites; φ_1 and φ_2 are the volume fractions of solvent and polymer respectively; χ is the Flory-Huggins interaction parameter; R_g is the universal gas constant; T is the absolute temperature; and X is the ratio of the polymer molar volume to that of the solvent

$$X = \left(M_2 / \rho_2 \right) / \left(M_1 / \rho_1 \right) \tag{33}$$

UCST phase behaviour is well accounted for by the Flory-Huggins theory with the interaction parameter χ exhibiting the following temperature dependence (McGuire *et al*, 1994):

$$\chi = A + B/T \tag{34}$$

where A and B are adjustable constants. The Flory-Huggins theory predicts the following for the critical value of the interaction parameter

$$\chi_c = 0.5 \left(1 + \sqrt{1/X} \right)^2 \tag{35}$$

The point where the binodal and spinodal curves intersect is determined by

$$\varphi_{2,c} = \frac{1}{1 + \sqrt{X}} \tag{36}$$

Unfortunately, the Flory-Huggins theory is unable to represent the phase envelopes in the vicinity of the critical temperature. However, Diekmann *et al* (2020) indicated that this theory does show the correct trends for the variation of the critical temperature with the molar mass of alkanes. Thus, another approach was considered.

2.4.2 Modelling the critical point

This Section reflects the discussion presented in Sitoe *et al* (2021).The Ising model was invented in 1920 as a mathematical model of ferromagnetism. The two-dimensional square-lattice Ising model is one of the simplest statistical models to show a phase transition (Gallavotti, 1999).

However, liquid-liquid phase separation of organic compounds shows characteristic features reminiscent of the 3D-Ising model (Domb, 1996). This is surprising, considering the simplicity of the Ising model which just considers entities located on a rigid three-dimensional lattice (Vale *et al*, 2010). These can assume one of two possible states and their interactions are limited to nearest neighbors. Such a system is capable of a phase transition, where the two phases differ with respect to the relative occupation of the two states. These are described by one single order parameter that distinguishes the different phases by assuming non-zero values for ordered states and vanishes when passing through a continuous phase transition.

When applied to liquid-liquid phase separation, the relative occupation of the two states in the Ising model is identified with a suitable composition variable, for example the volume- or the mole fraction. Near the UCST, T_c, the differences in the compositions of the coexisting phases can be represented by a power series in the reduced temperature (Schröer and Vale, 2009):

$$\tau = \left| T - T_c \right| / T_c \tag{37}$$

Renormalisation group theory led to the following expression for the shape of the coexistence curve (Aizpiri *et al*, 1992):

$$z_R - z_L = B\tau^{\beta} + B_1\tau^{\beta+\Delta} + B_2\tau^{\beta+2\Delta} + \ldots \tag{38}$$

where $\beta = 0.326$ and $\Delta = 0.50$ are universal critical exponents (Kumar *et al*, 1983); the B_i are system-dependent critical amplitudes; z_c, is the critical value of the composition variable z that defines the order parameter $z_R - z_L$, and the subscripts R and L refer to the right and left branches of the coexistence curve, respectively.

Singh and Pitzer (1989) suggested that the amplitude of the first correction-to-scaling term in Equation (38) universally assumes the value $B_1 \approx 0$ in fluid mixtures. Therefore, it is common

practice to only retain the leading term in Equation (38), with the others considered negligible (Vale *et al*, 2010):

$$z_R - z_L = B\tau^{\beta} \tag{39}$$

There is a noticeable discrepancy between the Ising phase diagram and those for real binary liquid-liquid systems. Unlike the phase diagrams predicted by the former, those for real fluids are generally asymmetric. The average composition of the two phases, termed the diameter, is not constant but varies with temperature. Mean field models, e.g., the van der Waals equation, predict that the diameter of the phase diagram varies linearly with the temperature near the critical point (Domb, 1996). This is known as the Cailletet-Mathias rectilinear diameter rule (Reif-Acherman, 2010). However, recent theoretical work (Cerdeiriña *et al*, 2006) led to the conclusion that the diameter of the coexistence curve, in general, is a sum of a linear term and nonanalytical terms with critical exponents of $1 - \alpha$ and 2β, respectively, i.e.

$$d = (z_L + z_R)/2 = z_c + A_o\tau^{1-\alpha} + A_1\tau^{2\beta} + \ldots \tag{40}$$

where α = 0.110 is a universal critical exponent and the A_i, are system dependent critical amplitudes (Aizpiri *et al*, 1992).

It is not very clear which composition variable for binary liquid systems is preferred, i.e., mole fraction, mass fraction or volume fraction (Kumar *et al*, 1983). However, Vale *et al* (2010) pointed out that for different choices of the concentration descriptors, e.g., mole fraction or volume fraction, the relative importance of the terms in Equation (40) varies. Depending on the choice, it may even lead to apparent cancellation of the nonanalytic terms, so that the linear approximation would work well in many instances. Damay and Leclercq (1991) noted that the asymmetry of the coexistence curve in binary systems is primarily due to a difference in size between the components. Damay and Leclercq (1991) therefore proposed the rescaling of the concentration descriptor in order to achieve a symmetric shape for the phase envelope. If this is possible, it will allow use of Equation (39) only, i.e., it becomes unnecessary to correct for the asymmetry. This proved possible by applying the *q*-fractions concept from Equation (6). Consider the *q*-fraction for a binary mixture described by volume fractions

$$q_1 = \frac{\beta_1\varphi_1}{\beta_1\varphi_1 + \beta_2\varphi_2} \tag{41}$$

A revised composition variable can then be defined by factoring the coefficients as follows

$$z_1 = \frac{\varphi_1}{\varphi_1 + m\varphi_2}; \text{ and } z_2 = \frac{m\varphi_2}{\varphi_1 + m\varphi_2} \tag{42}$$

where m is an adjustable constant chosen such that the phase envelope, when plotted against z_1, is symmetric and defined by

$$z_1 = z_c \pm \frac{B}{2}\left(\frac{T_c - T}{T_c}\right)^{\beta} \tag{43}$$

This proposal put forward by Damay and Leclercq (1991), embodied in Equation (43) was implemented for the DEET-alkane mixtures reported presently.

2.5 Polynomial expressions for physical property data

2.5.1 Scheffé and Bernstein polynomials

As mentioned, it was found that theoretical and empirical mixture models for surface tension models featured a common Padé-like structure (Dzingai *et al*, 2024). This opened a new window which suggested that, perhaps rational polynomial expressions would also apply to fit other mixture property data.

The classic way to approximate functions is via Taylor polynomials which were introduced in 1715 by Brook Taylor. They are generated by truncating the Taylor series expansion of a function $f(x)$ around point a.

$$f(x) = \sum_{n=0}^{\infty} \frac{f^{(n)}(x)}{n!}(x-a)^n \tag{44}$$

This can also be applied to multivariable functions, such as a binary mixture of x_1 and x_2. Consider a second order Taylor polynomial about the point (a, b):

$$\begin{aligned} f(x_1, x_2) = {} & f(a,b) + (x_1 - a)\frac{\partial f}{\partial x_1}(a,b) + (x_2 - b)\frac{\partial f}{\partial x_2}(a,b) + \\ & \frac{1}{2!}\left[(x_1 - a)^2 \frac{\partial^2 f}{\partial x_1^{\,2}}(a,b) + 2(x_1 - a)(x_2 - b)\frac{\partial^2 f}{\partial x_1 \partial x_2}(a,b) + (x_2 - b)^2 \frac{\partial^2 f}{\partial x_2^{\,2}}(a,b)\right] \end{aligned} \tag{45}$$

Obviously, this is a very tedious way of representing functions. Secondly, the approximation error of a Taylor expansion may increase rapidly further away from the approximation point. While these polynomials are generated for a function over $x \in \mathbb{R}$, they approach *f*(*x*) over a wider interval as *n* increases. Thirdly, it is not clear around which specific point this should be evaluated. The point (0, 0), which would define Equation (44) as a Maclaurin series, does not exist for a real mixture. In other words, it does not take the simplex constraint (mentioned in Section 2.1) into consideration. Consider for a binary mixture, a convenient starting point, e.g., (0.5, 0.5) where the function and its partial derivatives have a constant value. By gathering the similar terms in Equation (45), coefficients can be reassigned as

$$f(x_1, x_2) = \beta_0 + \beta_1 x_1 + \beta_2 x_2 + \beta_{11} x_1^{\,2} + \beta_{12} x_1 x_2 + \beta_{22} x_2^{\,2} \tag{46}$$

It was noted that the β_0 term could be multiplied by (x_1 + x_2), which is equal to unity. Reassignment of the coefficients then gives

$$f(x_1, x_2) = \beta_1 x_1 + \beta_2 x_2 + \beta_{11} x_1^{\,2} + \beta_{12} x_1 x_2 + \beta_{22} x_2^{\,2} \tag{47}$$

If the quadratic terms are expanded using $x_i^{\,2} = x_i(1 - x_j) = x_i - x_i x_j$, the second order Scheffé S-polynomial for a binary system is obtained, again with reassigned coefficients

$$S_2(2) = \beta_1 x_1 + \beta_2 x_2 + \beta_{12} x_1 x_2 \tag{48}$$

For experimental design, it is standard to apply Scheffé S-polynomials. The canonical model forms for *q* components in a mixture of orders (degrees) one, two and three are, respectively (Focke and Du Plessis, 2004; Scheffé, 1958):

$$S_q(1) = \sum_{i=1}^{q} \beta_i x_i \tag{49}$$

$$S_q(2) = \sum_{i=1}^{q} \beta_i x_i + \sum\sum_{i<j}^{q} \beta_{ij} x_i x_j \tag{50}$$

$$\begin{aligned} S_q(3) = & \sum_{i=1}^{q} \beta_i x_i + \sum\sum_{i<j}^{q} \beta_{ij} x_i x_j + \sum\sum\sum_{i<j<k}^{q} \beta_{ijk} x_i x_j x_k \\ & + \sum\sum_{i<j}^{q} \gamma_{ij} x_i x_j (x_i - x_j) \end{aligned} \tag{51}$$

An alternative but equivalent representation to these is the Scheffé K-polynomials (Draper and Pukelsheim, 1998). The second order Scheffé K-polynomial for a binary system, as analogue to Equation (47) is

$$K_2(2) = c_{11}x_1^{\,2} + 2c_{12}x_1x_2 + c_{22}x_2^{\,2} \tag{52}$$

In general, the nomenclature for the K-polynomials is given by $K_q(n)$, where q is the order of the homogenous polynomial and m indicates the number of components in the mixture. One very attractive property of K-polynomials is that they are readily extended to ternary and higher multicomponent mixtures. They were originally established by Kronecker algebra of vectors and matrices, but here a new way to generate them is laid out using Bernstein basis polynomials.

Sergei Bernstein developed Bernstein basis polynomials, as they are now called (Bernstein, 1912). They were developed as part of his proof of the Weierstrass Approximation Theory, which states (Duren, 2012: 151; Weierstrass, 1885):

> *If a function $f(x)$ is continuous on a closed bounded interval $[a, b]$, then for each $\varepsilon > 0$ there exists a polynomial $P(x)$ such that $|f(x) - P(x)| < \varepsilon$ for all x in $[a, b]$.*

In other words, every continuous function can be approximated uniformly by polynomials. The Bernstein basis polynomials of degree n form a complete basis over the interval [0,1] and the bases are defined by (Bernstein, 1912; Duren, 2012: 157):

$$b_{k,n} = \binom{n}{k} x^k (1-x)^{n-k} \tag{53}$$

Here, the binomial coefficient is defined by

$$\binom{n}{k} = \frac{n!}{k!(n-k)!} \tag{54}$$

and 0! = 1. Furthermore, if f is a continuous function on the interval [0, 1], then the Bernstein polynomial

$$B_n(f)(x) = \sum_{k=0}^{n} f\left(\frac{k}{n}\right) b_{k,n}(x) \tag{55}$$

will converge uniformly on [0, 1] as $n \to \infty$; in other words (Lorentz, 1953):

$$\lim_{n\to\infty} B_n(f) = f \tag{56}$$

Bernstein polynomials are a class of orthogonal polynomials. Orthogonal polynomials have the advantage that they can distribute the error over the interval of interest uniformly (Bellman, 1968: 194). If there is a sequence of polynomials $\{P_n(x)\}_{n=0}^{\infty}$, $P_n(x)$ of degree n, such that

$$(P_m, P_n) = \int_a^b P_m(x)P_n(x)w(x)dx = \delta_{mn}c_n \tag{57}$$

where $w(x)$ is the weighting function and δ_{mn} is the Kronecker delta (Weisstein, 2024):

$$\delta_{nm} \equiv \begin{cases} 0, & \text{for } m \neq n \\ 1, & \text{for } m = n \end{cases} \tag{58}$$

then $\{P_n(x)\}$ is an orthogonal polynomial sequence with respect to the weight function w on (a, b) (Chihara, 1978: 2). If $c_n = 1$, then the polynomials are not only orthogonal, but orthonormal as well. Many other orthogonal polynomials exist and can be used to approximate functions, such as Legendre polynomials, Hermitic polynomials or Chebyshev polynomials (Weisstein, 2024). Function approximation using these polynomials is done by first choosing the highest order version and then using a linear combination of all those polynomials up to that order over an interval specific to that polynomial. However, Bernstein basis polynomials are different as they are defined in the interval [0, 1] which provides an alternative and elegant way of representing binary systems. Since $x_2 = 1 - x_1$, Equation (55) can be rewritten as

$$B_n(x) = \sum_{k=0}^{n} \theta_{k,n} \binom{n}{k} x_1^{\,k} (x_2)^{n-k} \tag{59}$$

where the $\theta_{k,n}$ are adjustable constants. In the case of $n = 1$, i.e., a first order polynomial, this gives the linear blending rule

$$B_1(x) = \theta_{11}x_1 + \theta_{01}x_2 \tag{60}$$

For $n = 2$,

$$B_2(x) = \theta_{22}x_1^{\,2} + 2\theta_{12}x_1x_2 + \theta_{02}x_2^{\,2} \tag{61}$$

And for $n = 3$,

$$B_3(x) = \theta_{33}x_1^3 + 3\theta_{23}x_1^2x_2 + 3\theta_{13}x_1x_2^2 + \theta_{03}x_2^3 \tag{62}$$

Comparison of Equation (52) to Equation (62) shows that for binary mixtures, the K-polynomials and the Bernstein polynomials are identical. This also extends to the multivariate forms. The K-polynomials are homogeneous (i.e., all its terms have the same degree), and the corresponding information matrix is well-conditioned. Improvement of the conditioning of the information matrix generally reduces the variances of individual estimated regression coefficients, reduces the correlations between the variables, and makes the model less dependent on the precise location of the measurement data points (Prescott *et al*, 2002). The extension of the Bernstein basis polynomials to multicomponent mixtures is possible, but not part of this scope. Nevertheless, the quotient of two Scheffé K-polynomials creates Padé expressions that are useful for modelling mixture property data (Focke and Du Plessis, 2004).

As mentioned previously, some of the binary models for refractive index are Padé-type expressions. The concept of Padé approximants was formulated at the end of the 19th century within the classical theory of continued fractions (Frobenius, 1881; Padé, 1892). A rational function is the ratio of two polynomials. A Padé approximation is simply the rational function analogue of the Taylor series. Formally, a Padé approximation of order (m, n) to a function f at point a is defined as a rational function P_n/Q_m such that for x near a

$$\left|\frac{f(x) - P_n(x)}{Q_m(x)}\right| = O\left(\left(x-a\right)^{\nu}\right) \tag{63}$$

with ν as large as possible (Borowski and Borwein, 2005). In simpler terms, the (m, n) Padé approximation for a rational function is:

$$f(x) \cong \frac{\sum_{m=0}^{m} \kappa_m x^m}{\sum_{n=0}^{n} \lambda_n x^n} \tag{64}$$

or more explicitly (Andrianov and Shatrov, 2021):

$$P(m,n) = \frac{\kappa_0 + \kappa_1 x + \kappa_2 x^2 + \cdots + \kappa_m x^m}{\lambda_0 + \lambda_1 x + \lambda_2 x^2 + \cdots + \lambda_n x^n} \tag{65}$$

where the κ_i's and λ_i's are the regression coefficients of the polynomials. These types of functions have many applications in control theory (Seborg *et al*, 2011). It is not clear how Equation (65) can be extended to multicomponent systems. However, this dilemma is resolved by using the ratio of two Scheffé K-polynomials (Focke and Du Plessis, 2004):

$$P(m,n) = K_q(m) / K_q(n) \tag{66}$$

However, this functional form is also useful and prevalent for describing compositional variance in chemical properties such as surface tension (Dzingai *et al*, 2024), excess Gibbs free energy (Focke and Du Plessis, 2004), density, and viscosity. Another advantage is that if data for only two of the three binaries of a ternary system are available, this suffices to fit all the parameters of the $P(1,1)$ Padé model. This derivation is shown in Appendix A.2.

2.5.2 Projection functions leading to Scheffé polynomials

This Section reflects the contents of an article submitted for review by Pretorius *et al* (2024). It describes a novel extension of the Scheffé- and Padé-type expressions in the context of projections of pure component behaviour onto the simplex region.

Consider a single-phase liquid mixture of m different compounds at equilibrium at temperature T. The composition of a mixture is described by the vector of mole fractions: $\boldsymbol{x}^{\mathrm{T}} = (x_1, x_2, \ldots, x_n)$. It is postulated that the value which the physical property (p) of this multicomponent mixture assumes, is determined by a weighted average over the pure component property values (p_i), such as

$$p(\boldsymbol{x}) = \sum f_i(\boldsymbol{x})\, p_i \tag{67}$$

The weighting function $f_i(x_1, x_2, \ldots, x_n)$ corresponds to a projection of the property values of pure component i, onto the simplex region. The projection function must satisfy the following mathematical consistency requirements

$$\lim_{x_i \to 0} f_i(\boldsymbol{x}) = 0 \;\; \forall i \tag{68}$$

$$\lim_{x_i \to 1} f_i(\boldsymbol{x}) = \beta_i \;\; \forall i \tag{69}$$

In other words, when a component is absent, it should not contribute to the mixture property at all. Additionally, when only one component is present, it must match *some* unique characteristic of the pure component, termed β_i.

An assumption of the proposed formulation is that the parameters embedded in the weighting function $f(\boldsymbol{x})$ are temperature and pressure independent. Here, an ansatz is introduced that the projection function has the form of a Padé-type approximant. Consider the following $P(3,3)$ Padé approximant defined by the ratio of two cubic polynomials as the most general Padé approximant for a multicomponent mixture

$$\sigma = \sum_i \beta_i x_i \sigma_i \left(\sum_j \kappa_{ij} x_j \right) \left(\sum_k \lambda_{ik} x_k \right) \Bigg/ \left[\sum_i \beta_i x_i \left(\sum_j \tau_{ij} x_j \right) \left(\sum_k \omega_{ik} x_k \right) \right] \tag{70}$$

Here σ and σ_i represent the material property (in this case, surface tension) of the mixture and of pure component i respectively; while the κ_{ij}, λ_{ik}, τ_{ij} and ω_{ik} are adjustable binary parameters. Unfortunately, Equation (70) is excessively parameter rich. There is one parameter for each pure component and eight per binary in the mixture. Also, the pure component characteristics, β_i's, are ill-defined. It would be advantageous if they could be associated with readily measurable quantities representative of the individual pure components.

Parameter reduction is possible by considering the constraints on the adjustable parameters. The second order and third order Scheffé polynomials are considered now.

A special form of the quadratic Scheffé model (cf. Equation (52) which is equivalent to Equation (61)) is obtained with a projection function defined by

$$f_i(\boldsymbol{x}) = x_i \sum \kappa_{ij} x_j \text{ with } \kappa_{ii} = 1 \ \forall \ i \tag{71}$$

For a ternary mixture the corresponding expression for the mixture model is

$$p = x_1 p_1 \left(x_1 + \kappa_{12} x_2 + \kappa_{13} x_3 \right) + x_2 p_2 \left(\kappa_{21} x_1 + x_2 + \kappa_{23} x_3 \right) + x_3 p_3 \left(\kappa_{31} x_1 + \kappa_{32} x_2 + x_3 \right) \tag{72}$$

In Equations (71) and (72), there are two independently adjustable parameters per binary, i.e., κ_{ij} and κ_{ji}. This contrasts with the conventional second order Scheffé polynomial as it features only one adjustable parameter per binary (Draper and Pukelsheim, 1998). A parameter reduction can be achieved if links between the κ_{ij} and the κ_{ji} can be established. Consider the

postulate that the property values of a ternary mixture can be described by a quadratic expression defined by the product of two linear polynomials, i.e.

$$p = \left(a_1 x_1 + a_2 x_2 + a_3 x_3\right)\left(b_1 x_1 + b_2 x_2 + b_3 x_3\right) \tag{73}$$

This expression can be expanded as

$$p = a_1 b_1 x_1 \left(x_1 + \frac{b_2}{b_1} x_2 + \frac{b_3}{b_1} x_3 \right) + a_2 b_2 x_2 \left(\frac{b_1}{b_2} x_1 + x_2 + \frac{b_3}{b_2} x_3 \right) + a_3 b_3 x_3 \left(\frac{b_1}{b_3} x_1 + \frac{b_2}{b_3} x_2 + x_3 \right) \tag{74}$$

Comparing Equation (74) with Equation (72)(87) reveals that the pure component property corresponds to the product $p_i = a_i b_i$. Additionally, note that the model parameters are now linked via the relation $\kappa_{ji} = 1/\kappa_{ij}$. Furthermore, it is clear that the specification $\kappa_{ii} = 1$ arises naturally. Applying these conditions to Equation (84) yields a quadratic Scheffé polynomial with just one adjustable parameter per constituent binary.

A special form of the cubic Scheffé model is obtained by defining the projection function as

$$f_i\left(\boldsymbol{x}\right) = x_i \sum \kappa_{ij} x_j \sum \lambda_{ij} x_j \tag{75}$$

Again, links between the parameters of this equation can be established by postulating that the property of the mixture is defined by the product of three linear polynomials. Consider again a ternary mixture as the illustrating example

$$p = \left(a_1 x_1 + a_2 x_2 + a_3 x_3\right)\left(b_1 x_1 + b_2 x_2 + b_3 x_3\right)\left(c_1 x_1 + c_2 x_2 + c_3 x_3\right) \tag{76}$$

This expression can be expanded as

$$\begin{aligned} p = {} & a_1 b_1 c_1 x_1 \left(x_1 + \frac{b_2}{b_1} x_2 + \frac{b_3}{b_1} x_3 \right)\left(x_1 + \frac{c_2}{c_1} x_2 + \frac{c_3}{c_1} x_3 \right) \\ & + a_2 b_2 c_2 x_2 \left(\frac{b_1}{b_2} x_1 + x_2 + \frac{b_3}{b_2} x_3 \right)\left(\frac{c_1}{c_2} x_1 + x_2 + \frac{c_3}{c_2} x_3 \right) \\ & + a_3 b_3 c_3 x_3 \left(\frac{b_1}{b_3} x_1 + \frac{b_2}{b_3} x_2 + x_3 \right)\left(\frac{c_1}{c_3} x_1 + \frac{c_2}{c_3} x_2 + x_3 \right) \end{aligned} \tag{77}$$

In this case, the pure component properties are defined by the product $p_i = a_i b_i c_i$ and it also holds that

$$\kappa_{ji} = 1/\kappa_{ij};\ \lambda_{ji} = 1/\lambda_{ij} \text{ and } \kappa_{ii} = \lambda_{ii} = 1 \tag{78}$$

Applying these relationships to the weighting function of Equation (75) generates a special form of the cubic Scheffé polynomial with just two adjustable binary coefficients. In addition, unlike the conventional cubic Scheffé polynomials, the ternary constants that arises in multicomponent mixtures are fully determined in terms of the binary parameters. This is a very useful property since model parameters can then be fixed, at least in principle, from knowledge of binary mixture behaviour. In other words, it will not be necessary to measure properties for ternary mixtures.

2.5.3 Padé approximants for physical properties

This idea of Padé approximants based on Scheffé polynomials can be applied to refractive indices. In an ideal solution, both the molar refraction R and the molar volume V, follow the linear blending rule with mole fractions as the composition descriptors, as elaborated in Section 2.3.2. This means that, for an ideal binary solution the following expression holds

$$N = \frac{R}{V} = \frac{R_1 x_1 + R_2 x_2}{V_1 x_1 + V_2 x_2} = \frac{V_1 x_1 N_1 + V_2 x_2 N_2}{V_1 x_1 + V_2 x_2} \tag{79}$$

Equation (79) suggests that, for the physical property N, the β_i's can be associated with the molar volumes (V_i) of the pure components at the temperature of the solution. The refractive index is subsequently recovered from the Lorentz-Lorenz parameter N via the expression

$$n = \sqrt{\frac{1+2N}{1-N}} \tag{80}$$

Alternatively, the refractive index of an ideal solution can be modelled via a $P(1,1)$ Padé approximant in which mass fractions serve as the composition descriptors. If this is done, an expression is obtained in which the molar mass M_i serves as a temperature-independent β_i surrogate. To achieve this, first define a new property

$$r \equiv N/\rho = R/M \tag{81}$$

The molar mass of the mixture is given by a linear combination of the molar masses of the components. For ideal solutions this also holds for the molar refraction. Therefore

$$r = \frac{R_1 x_1 + R_2 x_2}{M_1 x_1 + M_2 x_2} = \frac{M_1 x_1 \left(N_1/\rho_1\right) + M_2 x_2 \left(N_2/\rho_2\right)}{M_1 x_1 + M_2 x_2} = \frac{M_1 x_1 r_1 + M_2 x_2 r_2}{M_1 x_1 + M_2 x_2} \tag{82}$$

In other words, for ideal solutions, it holds that the parameter r is a mass fraction weighted average over the pure component values

$$r = r_1 w_1 + r_2 w_2 + r_3 w_3 \tag{83}$$

Equation (79) and Equation (82) are equivalent forms, but they use different data during the regression analysis. Therefore, there will be differences in the prediction errors. Conveniently, Equation (82) offers the advantage that all the parameters are temperature independent. However, the actual mixture density must be known in order to determine the value of the refractive index using

$$n = \sqrt{\frac{1+2\rho r}{1-\rho r}} \tag{84}$$

When using Equation (79) instead, it is only necessary to know the molar masses and the densities of the pure components as a function of temperature. Hence, it was chosen for this analysis.

2.6 Summary

Refractive indices provide a simple, temperature-dependent way to correlate compositional data, if a calibration curve is available. However, it is uncertain which type of composition variable to use. The phase equilibrium behaviour of polymer-solvent systems can be expressed by the Flory-Huggins model but requires a new type of composition variable for modelling the critical point. For mixtures, many of the mixing rules available can be seen as Padé-type expressions (ratios of polynomials). Yet it is unclear which set of regression coefficients and constraints would perform best. These unknowns are now addressed.

3 Materials and methods

3.1 Materials

In order to model the behaviour of polyethylene with DEET, a series of *n*-alkanes were used as short chain analogues to the polymer. Their details are given in Table 3. All the compounds were obtained from Merck and were used as received without further purification.

Table 3: Chemical details

Chemical	CAS #	Product code	Code	Purity, %
DEET	134-62-3			
Dodecane (C12)	112-40-3	101987112	297879	> 99
Hexadecane (C16)	544-76-3	101444299	296317	> 99
Eicosane (C20)	112-95-8	1002515748	219274	99
Tetracosane (C24)	641-31-1	1002801750	T8752	99
Octacosane (C28)	630-02-4	102200614	O504	99
Dotriacontane (C32)	544-85-4	102181345	D223107	97

3.2 Methods

3.2.1 Evaluation of mixing rules

Literature data for refractive index measurements on other alkanes and binary mixtures of these components with polar organic compounds were obtained. Table 4 lists the different systems considered together with their sources for the density and refractive index of pure components and binary mixtures. In a few cases, when the density of the pure component was not available, it was calculated using the correlation reported by Yaws and Pike (2009):

$$\rho = A B^{-(1-T/C)^n} \tag{85}$$

where *A*, *B*, *C*, and *n* are empirical constants.

Table 4: List of data sources for density and refractive index for pure components and binary mixtures

Pure compounds	Temperature range, °C	References
Dodecane	20–100	(Casás *et al*, 2002; Caudwell *et al*, 2004; Pardo *et al*, 2001; Paredes *et al*, 2012)
Hexadecane	20–60	(Queimada *et al*, 2005; Sirbu *et al*, 2019)
Eicosane	40–100	(Dutour *et al*, 2001; Queimada *et al*, 2005)
Tetracosane	60–100	(Queimada *et al*, 2005; Yaws and Pike, 2009)
Octacosane	50–100	(Yaws and Pike, 2009)
Dotriacontane	75–100	(Yaws and Pike, 2009)
Binary systems	**Temperature range, °C**	**References**
Acetone-alkanes	15–35	(Acosta *et al*, 2001; Casás *et al*, 2002; Marino *et al*, 2000; Marino *et al*, 2001)
Anisole-alkanes	20–30	(Calvar *et al*, 2009) (Al-Jimaz *et al*, 2005) (Orge *et al*, 2000)
Benzene-alkanes	10–40	(Calvar *et al*, 2009; Diaz Peña and Nuñez Delgado, 1975; Dymond and Young, 1981; González *et al*, 2010; Lal *et al*, 2000; Letcher, 1984; Ridgway and Butler, 1967; Teja and Rice, 1976)
Chlorobenzene-alkanes	25–35	(Gayol *et al*, 2010; Tourino *et al*, 2004)
Cyclohexanone-alkanes	25–35	(Aralaguppi *et al*, 1999)
Dioxane-alkanes	25–35	(Calvo *et al*, 1998; Nayak *et al*, 2003; Penas *et al*, 2000)
Ethanol-alkanes	15–45	(Blanco *et al*, 2013; Gayol *et al*, 2007; Jiménez *et al*, 2000; Orge *et al*, 1997; Orge *et al*, 1999; Segade *et al*, 2003)

3.2.2 Refractometry

Refractive index values were measured as a function of temperature using a Mettler Toledo R4 refractometer. The calibration of the instrument was checked using double distilled and deionised water in both a heating and cooling run. These values were compared to those of water in the literature (Bashkatov and Genina, 2003; Thormählen *et al*, 1985) as shown in Figure 2. The instrument precision was ± 0.0001 and repeatability was ± 0.0002 refractive index units.

Solid reagents were melted before being weighed out. All reagents were weighed on a Mettler Toledo analytical balance to four decimal places. The reagents were pipetted into small vials with screw tops and molecular sieves to entrap any atmospheric moisture. The vials and glass

pipettes were placed in the oven to ensure homogenous solutions right before measurements were taken.

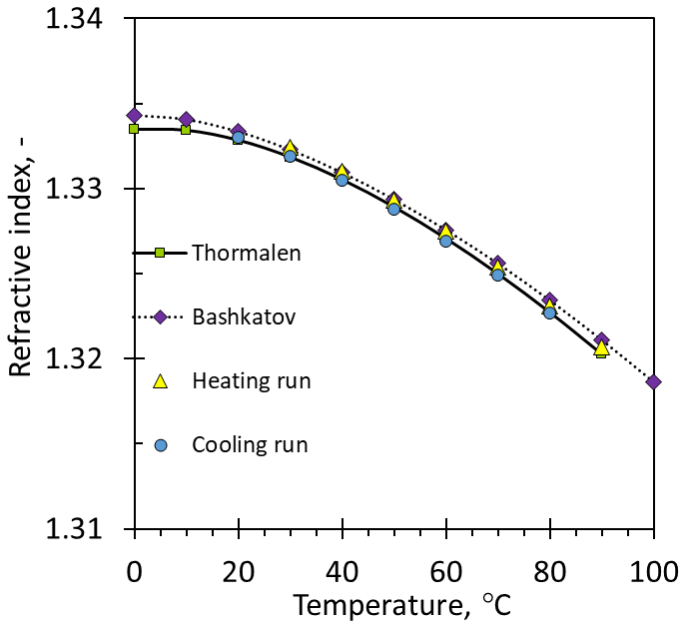

Figure 2: Water refractive index repeatability curve as compared to literature data (Bashkatov and Genina, 2003; Thormählen *et al*, 1985).

The refractometer sample holder is conical with a prism located in the bottom. Therefore, the refractive index is measured for the densest layer of sample fluid (i.e., that which is in direct contact with the flat surface). Sample amounts varying between 0.15 g and 0.5 g were weighed out and directly pipetted into the instrument cell. The measurements were conducted in decreasing temperature increments with time delays programmed into the device to ensure equilibrium was reached.

3.2.3 Determination of phase envelopes

The pure component molar mass, density, and refractive index as a function of temperature were used to determine the pure component molar refractivity. These values were then used along with the mixture refractive index to calculate the volume fraction of a component present in the mixture. As it cools, the composition locus should either follow the phase boundary or form a jump discontinuity to the other side. The method was applied to mixtures of DEET with a range of linear alkanes of increasing chain length, to finally extrapolate to the phase behaviour of polyethylene-DEET mixtures. The number average molecular mass of the polyethylene considered for making the anklets was 50.4 kDa.

Firstly, the liquid sample was prepared by accurately weighing out suitable quantities of the two components into the measurement cell. Again, the temperature was set at a high value and sufficient time was allowed before measuring the refractive index so that equilibrium was reached.

A check was done to justify the validity of the model. For this, the measured refractive index value was compared to the one predicted by Equation (19) by using Equation (80).

In the homogenous state, if the predicted composition matched the set values, the aforementioned assumptions and models were considered justified. The temperature was lowered by a few degrees, and the procedure was repeated. The locus of the refractive index, for a homogeneous liquid, follows a straight line if plotted against temperature and, on the temperature-composition plot, it is a vertical line. Once the boundary of a two-phase region is traversed, the locus of the measured refractive index deviates from these straight lines because the composition changes. Once this happened, sufficient time was allowed to ensure that the system reached a true equilibrium state. This took several minutes, and, in a few cases, it took more than an hour. The molar volume of the alkanes being tested was estimated using the density correlations reported by Yaws and Pike (2009). The apparent composition of the mixture was then estimated from Equation (24) and

$$x_1 = \varphi_1 V_2 / (\varphi_1 V_2 + \varphi_2 V_1) \tag{86}$$

The temperature was adjusted, and the process repeated. On further cooling, the composition locus should either follow a phase boundary curve or “jump” to the other branch of the phase envelope on the other side of the critical temperature.

3.2.4 Padé expression fitting

Data from the sources in Table 5 was extracted and used to fit Padé-type functions. System I (as designated by Pretorius *et al* (2024)) contained density but not refractive index measurements. Here a single temperature at which the analysis was done was chosen.

Table 5: Data sources of refractive index measurements of ternary systems

#	Ternary system	T (°C)[#]	References
II	diisopropyl ether, ethanol, and methylcyclohexane	25	(Ye and Tu, 2005)
III	acetone, ethanol, and 2,2,4-trimethylpentane	25	(Chen and Tu, 2005)
IV	ethanol, 2-methylpropan-2-ol, and 2,2,4-trimethylpentane	25	(Wang *et al*, 2005)
V	diisopropyl ether, ethanol, and 2,2,4-trimethylpentane	25	(Chen and Tu, 2006)
VI	tetrahydofuran, 2-propanol, and 2,2,4-trimethylpentane	25	(Ku *et al*, 2008)
VII	2-propanol, benzyl alcohol, and 2-phenylethanol	35	(Huang *et al*, 2008; Yeh and Tu, 2007)
VIII	1,3-dioxolane, 2-propanol, and 2,2,4-trimethylpentane	25	(Ku *et al*, 2009)
IX	2-propanol, tetrahydropyran, and 2,2,4-trimethylpentane	30	(Kao and Tu, 2011)
X	ethanol, benzyl acetate, and benzyl alcohol	30	(Chen *et al*, 2012)

As mentioned in Section 2.5.3, constraints on the parameters are preferred. The denominator polynomial must always exceed zero. Otherwise, negative values may be generated, and an undefined property value will arise. Further constraints can also be imposed to reduce the number of parameters to fit, and this concept was explored in depth in the article (Pretorius *et al*, 2024). Table 6 shows the different variations of the Padé projection models for ternary mixtures that were considered in the analysis. This includes the $P(2,2)$ model

$$p = \frac{\beta_1 x_1 p_1 \left(x_1 + \kappa_{12} x_2 + \kappa_{13} x_{23}\right) + \beta_2 x_2 p_2 \left(\kappa_{21} x_1 + x_2 + \kappa_{23} x_3\right) + \beta_3 x_3 p_3 \left(\kappa_{31} x_1 + \kappa_{32} x_2 + x_3\right)}{\beta_1 x_1 \left(x_1 + \lambda_{12} x_2 + \lambda_{13} x_{23}\right) + \beta_2 x_2 \left(\lambda_{21} x_1 + x_2 + \lambda_{23} x_3\right) + \beta_3 x_3 \left(\lambda_{31} x_1 + \lambda_{32} x_2 + x_3\right)} \tag{87}$$

and the $P(3,1)$ model

$$p = \sum_i \beta_i x_i \sum_j \kappa_{ij} x_j \sum_k \lambda_{ik} x_j \Big/ \sum_l \beta_l x_l \tag{88}$$

Note that the specific volume is given by $\upsilon_i = 1/\rho_i$.

Table 6: Padé-type projection model variants (based on parameter constraints)

***P*(2,2) model:**		
Binary parameters		
Model variant code	Parameter constraints	# Parameters*
Ideal	$\lambda_{ij} = \kappa_{ij} = 1$	0
A	$\lambda_{ij} = \kappa_{ij}$ & $\kappa_{ji} = 1/\kappa_{ij}$	1
B	$\lambda_{ij} = \kappa_{ij}$	2
C	$\lambda_{ji} = 1/\lambda_{ij}$ & $\kappa_{ji} = 1/\kappa_{ij}$	2
D	None	4
***P*(3,1) model:**		
Binary parameters		
Model variant code	Parameter constraints	# Parameters*
E	$\lambda_{ji} = 1/\lambda_{ij}$ & $\kappa_{ji} = 1/\kappa_{ij}$	2
F	None	4
Pure component descriptors		
Physical property	p_i for $\beta_i \equiv V_i$	p_i for $\beta_i \equiv M_i$
Refractive index	$N_i = \left(n_i^2 - 1\right)/\left(n_i^2 + 2\right)$	$N_i = \upsilon_i \left(n_i^2 - 1\right)/\left(n_i^2 + 2\right)$

*The number of adjustable parameters per binary in the mixture

The parameter values were fixed using least squares regression analysis executed in MS Excel. Results obtained using only the binary data for this purpose, and also when the full data sets were considered, are reported. The Akaike information criterion (AIC) (Akaike, 1983) was used to rank the relative performance of the models. The governing equation is

$$\mathrm{AIC} = n \ln(SSE) + 2df \tag{89}$$

where n is the number of data points, SSE is the sum of the square errors, and df is the degrees of freedom, i.e. the number of parameters that were fitted. To compare models, it is only the difference between the AIC values that matters. On taking differences, the units cancel out and the result is unitless

$$\Delta\mathrm{AIC} = n \ln(SSE_{\mathrm{ref}} / SSE_{\mathrm{model}}) + 2\Delta df \tag{90}$$

The cases employing $\beta_i = V_i$ and $\beta_i = M_i$ were considered separately. For each mixture property, the corresponding $P(1,1)$ Padé "ideal solution" expression served as the reference model. The obtained ΔAIC values were normalised by taking the ratio with respect to the largest value recorded. The normalised ΔAIC values, obtained when regressing just the binary data, were compared to the values obtained when the full data set were used instead.

4 Results and discussion

4.1 Refractometry mixing rules

4.1.1 Single compounds

The measured refractive indices of the pure *n*-alkanes considered are plotted in Figure 3. For any fixed temperature, the refractive index increases with alkane chain length. The temperature dependence was perfectly linear over the full measurement range, i.e., it could be represented by

$$n(T) = n^o + m\left(T - T^o\right) \tag{91}$$

where $n°$ is the refractive index of the compound at the reference temperature $T°$ and m is the slope of the refractive index line when plotted against temperature.

Figure 4(a) shows data plots of the molar refraction, R, calculated from Equation (12) with refractive index and density data extracted from the sources listed in Table 4. The scaled molar refraction R/M data are reported in Figure 4(b). The results substantiate the temperature-independence of the molar refraction, and the molar mass scaled version as expressed by Equation (14), in the case of *n*-alkanes. The R/M values observed in Figure 4(b) are very close to one third. Nevertheless, the data trends suggest a very weak linear temperature dependence. In the temperature range displayed, the R/M values, as well as the temperature slope, decrease with alkane chain length. The slope is positive for dodecane, hexadecane and eicosane but negative for the longer alkane members. However, the variation with temperature, in the range considered, is negligible as it amounts to less than ± 0.2 %. For all practical purposes, the molar refraction values, R, may therefore be assumed to be constants.

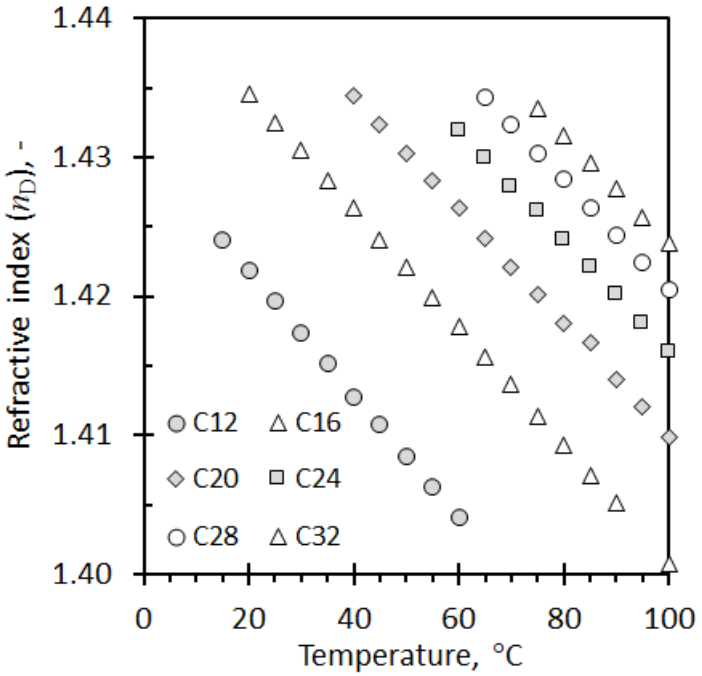

Figure 3: Measured refractive index values for measured for selected linear *n*-alkanes: C12: Dodecane; C16 Hexadecane; C20 Eicosane; C24 Tetracosane; C28 Octacosane and C32 Dotriacontane.

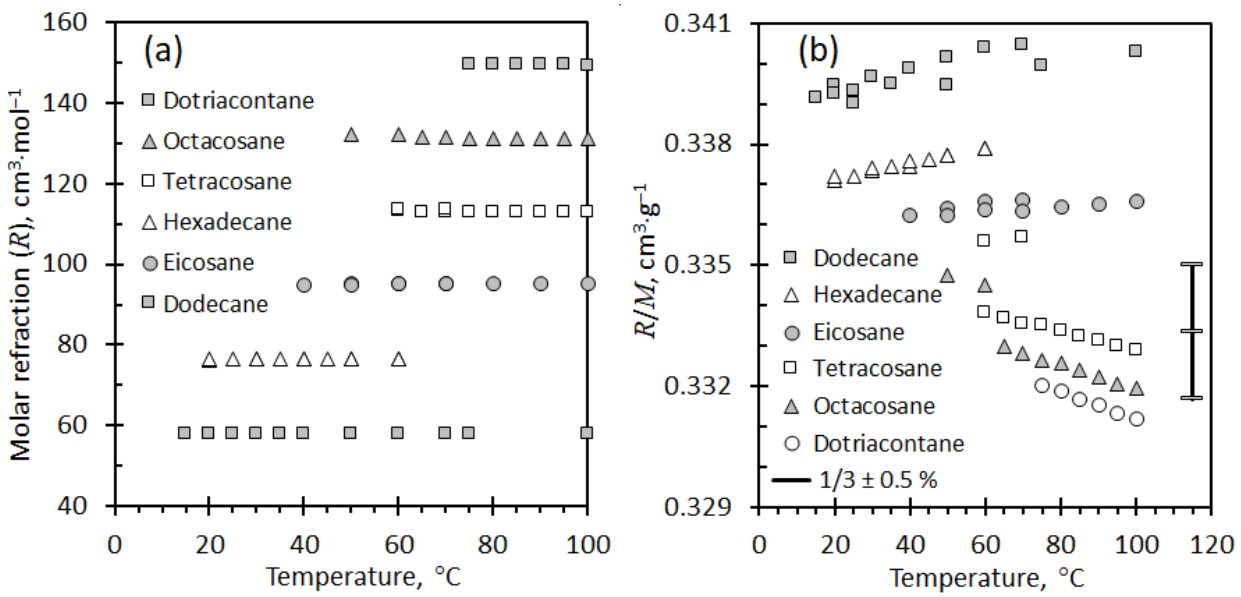

Figure 4: Data for (a) the molar refraction *R*, and (b) the molar-mass scaled form *R*/*M* for selected alkanes in the liquid state. The scale bar in (b) shows a ± 0.5 % deviation from one third.

If this is the case, the Lorentz–Lorenz relationship of Equation (14) allows the calculation of the liquid density from refractive index measurements.

$$\rho = \frac{M}{R}\left(\frac{n^2-1}{n^2+2}\right) = \frac{M}{R}N \tag{92}$$

The applicability of this approach was tested on the *n*-alkanes together with data for some additional compounds. The results are summarised in Table 7. Experimental values for the densities and refractive indices over certain temperature ranges were obtained from the literature as per Table 4. These values were used to calculate the molar volume and molar refraction at each data point. The calculated values obtained were averaged over the whole temperature range. Subsequently, the mean value for R obtained for each component was used to calculate its density over the temperature range considered with Equation (92). Table 7 lists the R values and the mean and maximum absolute average deviations (AAD) for the density prediction errors obtained by applying Equation (92). Table 7 indicates that the molar refraction is less affected by the system temperature than the molar volume. The standard deviation (s), expressed as a relative percentage, averaged 0.14 % for R and 1.14 % for the molar volume over the temperature ranges considered. The variation in R is therefore almost order of magnitude smaller in value compared to V.

The Looyenga and modified Eickman models were also investigated. This was done by replacing the expression for N, *i.e.* $(n^2\text{-}1)/(n^2\text{+}2)$, in the Lorentz-Lorenz expression with either $n^p - 1$ or with $(n^2\text{-}1)/(n^2\text{+}d)$, respectively. Setting $p = 2/3$ or $d = 0.4$ resulted in slightly larger standard deviations in the R values compared to the Lorentz-Lorenz approach. Only minor improvements were observed when allowing these adjustable parameters to vary. At best, the performance was the same as for the Lorentz-Lorenz equation. Surprisingly, the results were rather insensitive to the actual values assigned to the parameters d and p. Density predictions covered a wide range of values and agreed, on average, within 0.2 %, with a maximum deviation of less than 1 %. Subsequently, Equation (92) proves to be applicable for calculating pure component temperature-dependent density values in the absence of experimental data or correlations—provided that at least a single density point at a reference temperature is available to allow for the calculation of R. This is useful in correlations where pure component density data are required to predict the mixture composition and only refractive index measurements are available.

Table 7: Pure components: Average values of the molar volumes and molar refractions with the density predicted from *R*

	T-range,	Molar volume, $cm^3 \cdot mol^{-1}$				Lorentz-Lorenz molar refraction, $cm^3 \cdot mol^{-1}$				Density errors	
Compound	°C	*V*	±	*s*	*s*, %	*R*	±	*s*	*s*, %	Max %	AAD %
Benzene	8–50	89.9	±	1.28	1.43	26.22	±	0.04	0.16	0.28	0.15
Acetone	20–45	74.3	±	1.20	1.61	16.16	±	0.04	0.23	0.43	0.15
DMA	25–45	94.0	±	0.94	1.00	24.34	±	0.02	0.09	0.09	0.06
Anisole	20–30	109.3	±	0.52	0.47	32.93	±	0.07	0.22	0.24	0.16
Cyclo-hexanone	25–35	104.7	±	0.51	0.49	27.93	±	0.01	0.05	0.05	0.03
Dioxane	25–35	86.2	±	0.48	0.56	21.69	±	0.01	0.06	0.07	0.04
Ethanol	15–45	59.1	±	0.71	1.19	12.91	±	0.01	0.05	0.08	0.04
Dodecane	20–100	232.7	±	5.88	2.53	57.86	±	0.08	0.14	0.23	0.12
Hexadecane	20–60	297.9	±	3.73	1.25	76.43	±	0.06	0.08	0.12	0.07
Eicosane	40–100	373.1	±	6.09	1.63	95.06	±	0.04	0.04	0.06	0.03
Tetracosane	60–100	442.1	±	4.26	0.96	113.0	±	0.33	0.29	0.58	0.21
Octacosane	50–100	509.3	±	5.21	1.02	131.4	±	0.39	0.29	0.56	0.22
Dotriacontane	75–100	580.4	±	3.76	0.65	149.5	±	0.14	0.09	0.12	0.07
Average (max)					1.14				0.14	(0.58)	0.10

4.1.2 Binary mixtures containing an *n*-alkane

Figure 5 shows that all the binary mixtures of acetone with alkanes appear to behave like ideal mixtures with respect to both the molar refraction and the molar volume. This also holds for other compounds in mixtures with *n*-alkanes as demonstrated by Figure 6 to Figure 9. Note on Figure 7 the curvature of the *V* vs. x_1 lines. The molar volume of benzene (as $x_1 \rightarrow 1$) in mixtures with hexane and heptane deviates from that seen with the other *n*-alkanes, namely 90 $cm^3 \cdot mol^{-1}$. Moreover, the other figures indicate that the molar volumes for *n*-hexane and *n*-heptane are around 130 $cm^3 \cdot mol^{-1}$ and 148 $cm^3 \cdot mol^{-1}$ respectively. This indicates a useful feature of this approach, *viz*. to determine when reported measurements are likely faulty.

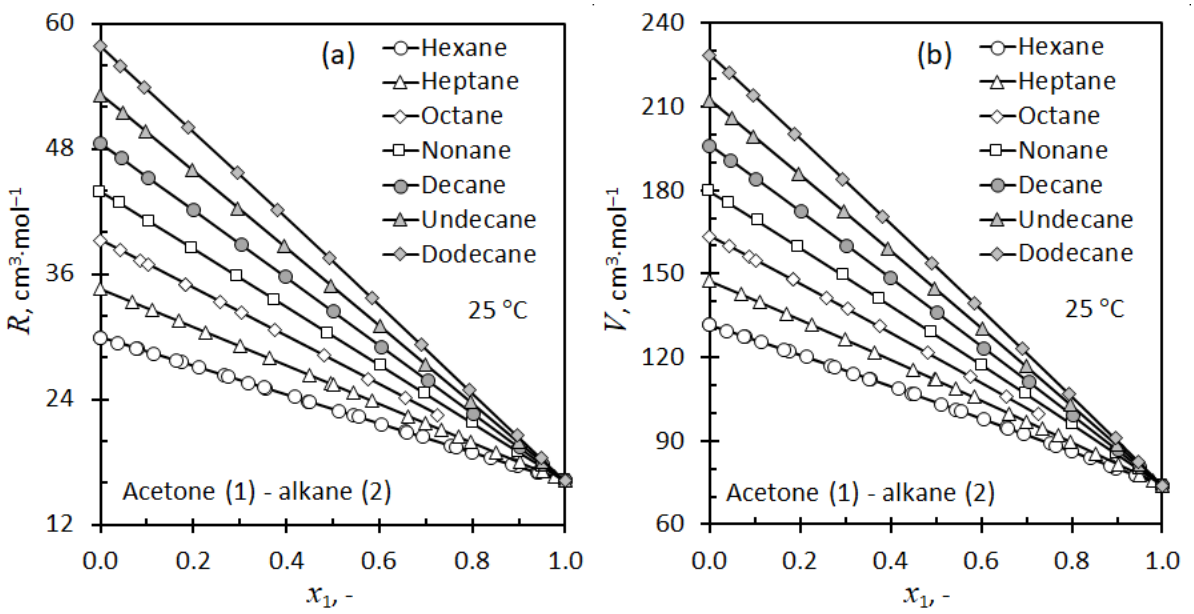

Figure 5: The Lorentz-Lorenz molar refraction R and molar volume at 25 °C for binary mixtures of acetone with selected alkanes calculated using the data sources listed in Table 4.

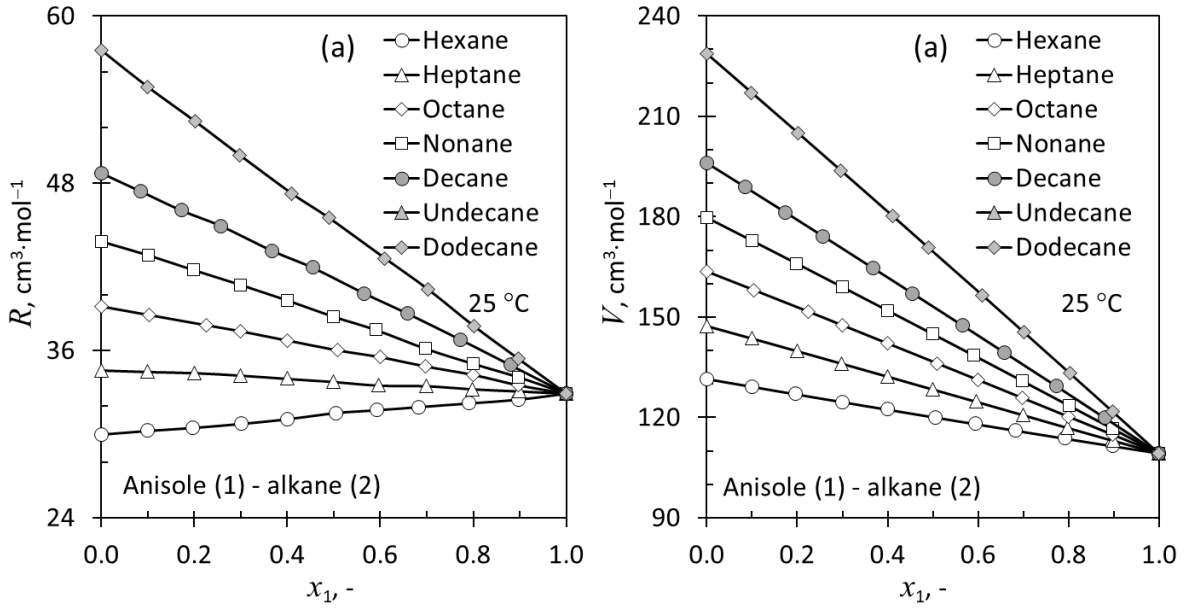

Figure 6: The Lorentz-Lorenz molar refraction R and molar volume V at 25 °C for binary mixtures of anisole with selected alkanes calculated using the data sources listed in Table 4.

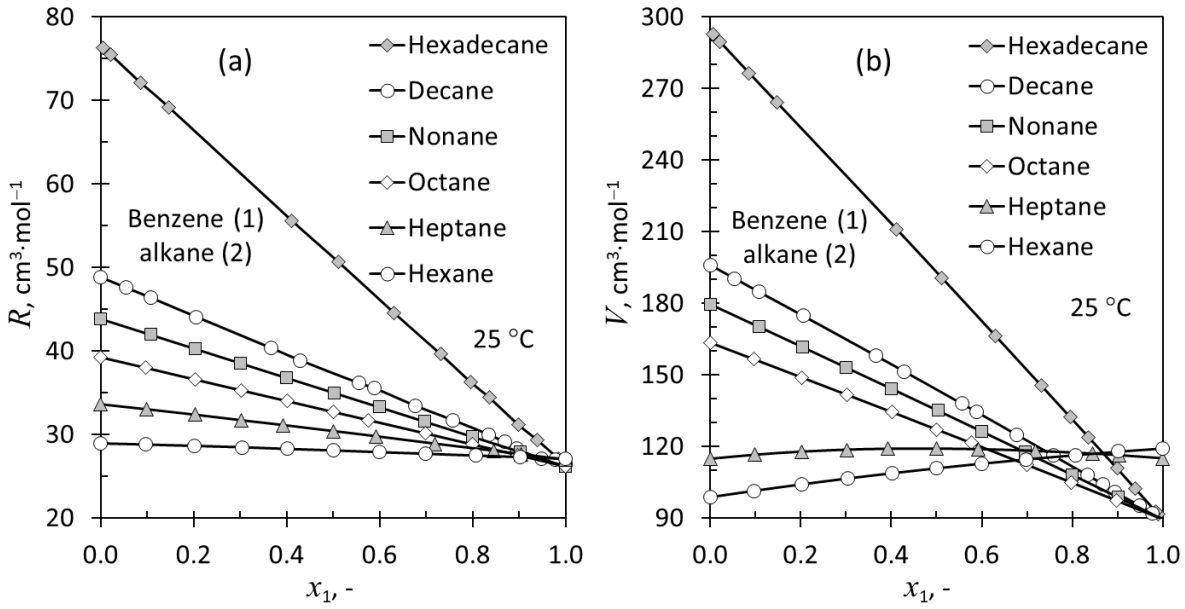

Figure 7: The Lorentz-Lorenz molar refraction *R* and molar volume *V* at 25 °C for binary mixtures of benzene with selected alkanes calculated using the data sources listed in Table 4.

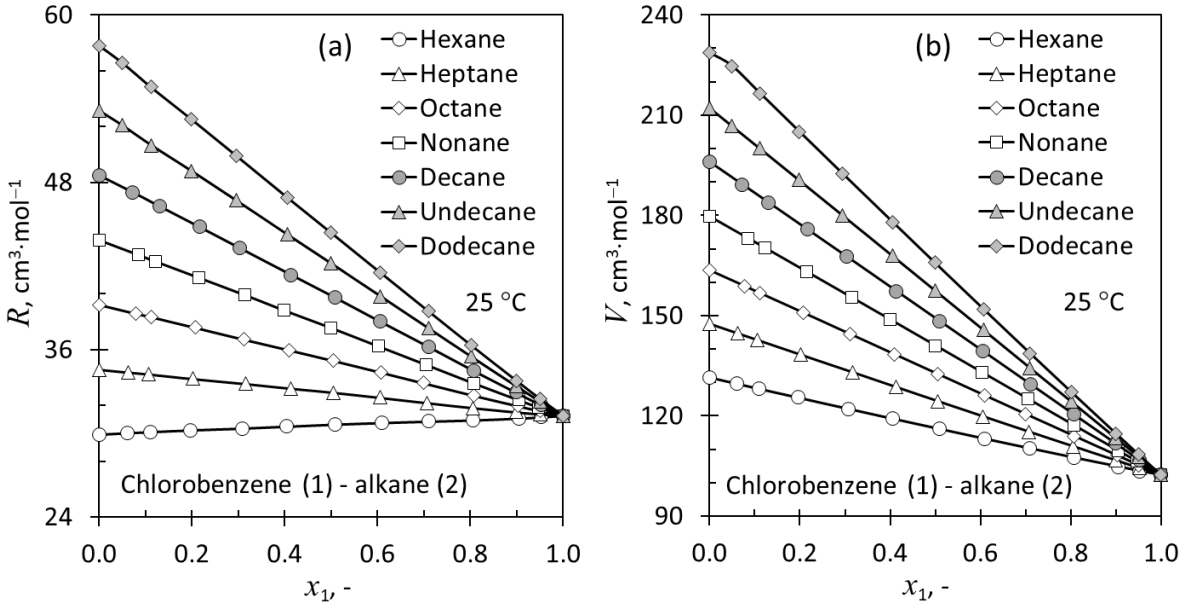

Figure 8: The Lorentz-Lorenz molar refraction *R* and molar volume *V* at 25 °C for binary mixtures of chlorobenzene with selected alkanes calculated using the data sources listed in Table 4.

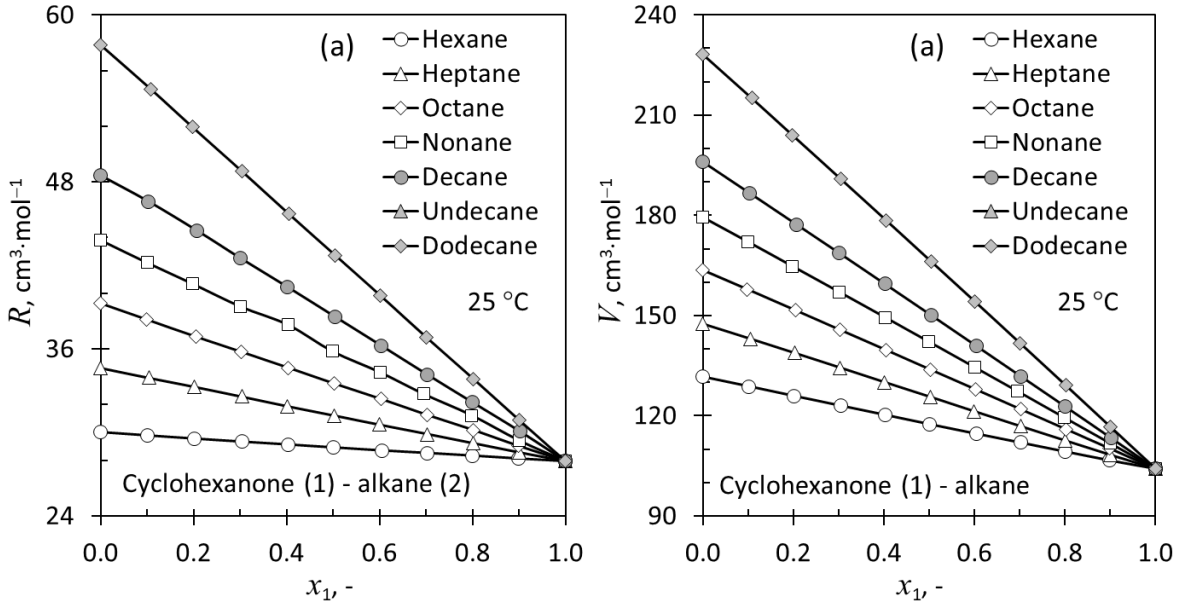

Figure 9: The Lorentz-Lorenz molar refraction R and molar volume V at 25 °C for binary mixtures of cyclohexanone with selected alkanes calculated using the data sources listed in Table 4.

Figure 10 shows the temperature dependence of the molar refraction and the molar volume for mixtures of 1,4-dioxane with *n*-hexane. The R data for measurements conducted at temperatures of 25 °C, 30 °C and 35 °C, all lie on the same straight line. However, the corresponding molar volume data values lie on three separate parallel lines. Similar observations were made for the other binary systems listed in Table 4. Figure 11 confirms this for ethanol mixtures with *n*-alkanes as well. This confirms the notion that the molar refraction can be interpreted as a temperature-invariant scaled molar volume. The results presented above appear to be generally valid for alkanes in binary combinations with aromatic and/or polar compounds such as benzene, chlorobenzene, ethanol, anisole, cyclohexanone, and 1,4-dioxane. The key conclusion from these results is that the molar refraction R varies linearly with composition expressed in terms of mole fractions and that it is, for practical purposes, temperature invariant.

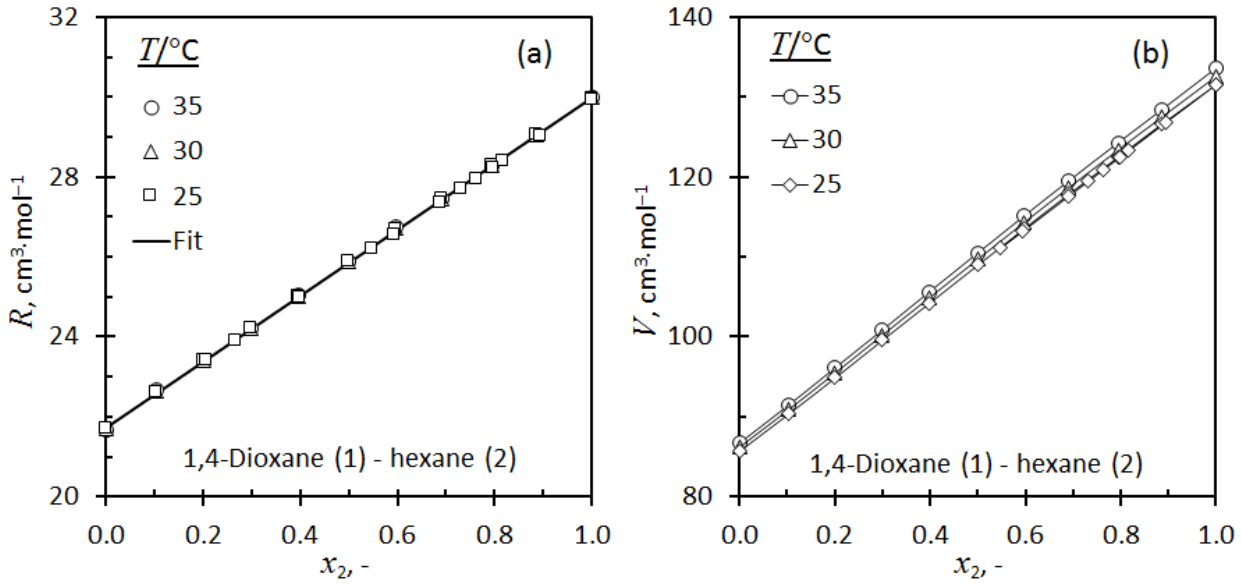

Figure 10: The temperature dependence of the Lorentz-Lorenz molar refraction R and molar volume for binary mixtures of 1,4-dioxane with *n*-hexane

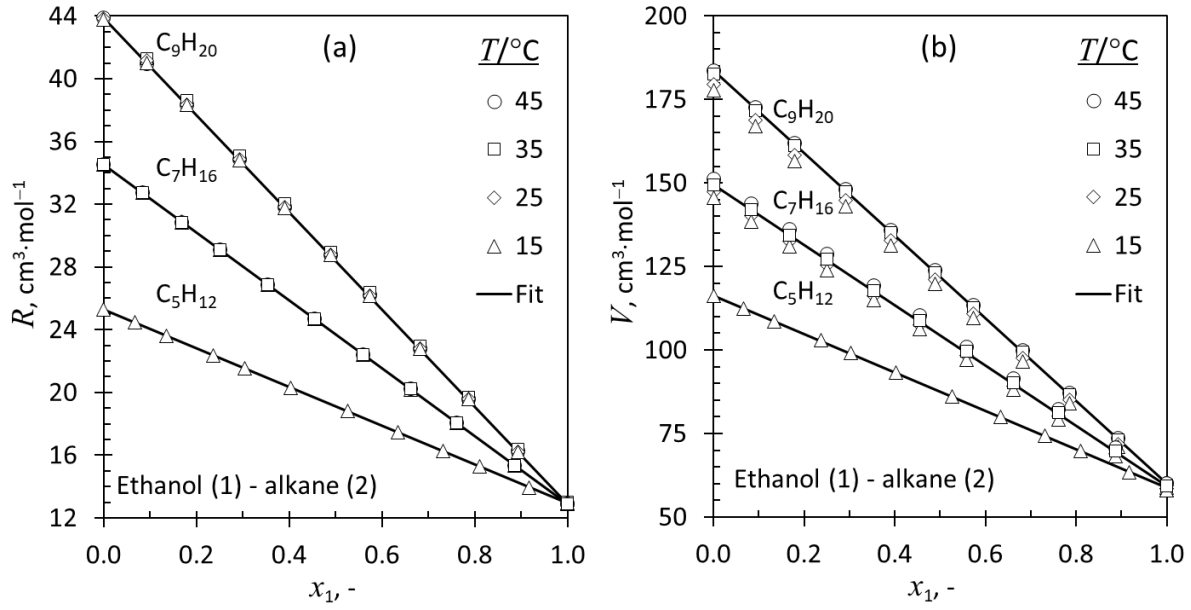

Figure 11: The temperature dependence of the Lorentz-Lorenz molar refraction R and molar volume V for binary mixtures of ethanol with pentane or heptane or nonane.

Next, the different mixing rules presented in Table 2 were compared. The models with a linear composition dependence fall in two groups corresponding to whether the mole fractions or the volume fractions are used as the composition descriptors, namely

$$g(n) = g(n_1)x_1 + g(n_2)x_2 \tag{93a}$$

and

$$f(n) = f(n_1)\varphi_1 + f(n_2)\varphi_2 \tag{93b}$$

where $g(n_i)$ and $f(n_i)$ represent the functional dependence of the parameter N on refractive index suggested by the different investigators as listed in Table 2. These equations can be rearranged in a format that facilitates plotting all data from all systems on a single graph. This method also allows the complex Heller and Wiener mixture laws to be compared by

$$X \equiv \frac{g(n) - g(n_1)}{g(n_2) - g(n_1)} = x_2 \tag{94a}$$

and

$$\Phi \equiv \frac{f(n) - f(n_1)}{f(n_2) - f(n_1)} = \varphi_2 \tag{94b}$$

It should be noted that a volume fraction is an ill-defined concept because only nominal values based on the pure component properties are used. The true volume of the mixture differs slightly from the molar volume calculated using the linear mixing rule due to non-ideal mixing. Mole fractions are therefore preferred. If the model is able to represent the experimental data, the plots of Φ vs. φ_2 or of X vs. x_2 should yield a straight line with slope of unity that passes through the origin. Figure 12(a) shows that this is indeed the case for Equation (15) and Equation (18a) on plots against the mole fraction. This means that the molar volume and the Lorentz-Lorenz molar refraction measured, for all the systems considered presently, do follow the linear mixing rule with mole fraction as the composition descriptor.

Figure 12(b) shows the plots of the models that are based on linear expressions in the volume fractions. Interestingly, all of the mixture models return data pairs that are very close to each other. The differences were smaller than the size of the symbols used to denote them and lie on top of each other in the graph. Unfortunately, none of them are able to correlate the data from all systems. This is indicated by the considerable scatter of the data points at distances quite far away from the diagonal line. The plot of the data from the 1,4-dioxane-decane binary appears to represent the greatest deviations. These data points were calculated using the weighted power mean equation and they are highlighted in the red squares that are connected with a solid line. It is clear that this data set cannot be represented by any of the models tested in Figure 12(b). The calculations even yield Φ values that exceed unity. This is in stark contrast with the results shown in Figure 12(a) where the 1,4-dioxane-decane data fall precisely on the required straight line when the models based on mole fraction are used. Interestingly, it did not matter whether the Lorentz-Lorenz or Looyenga expression for N was used. The results were identical.

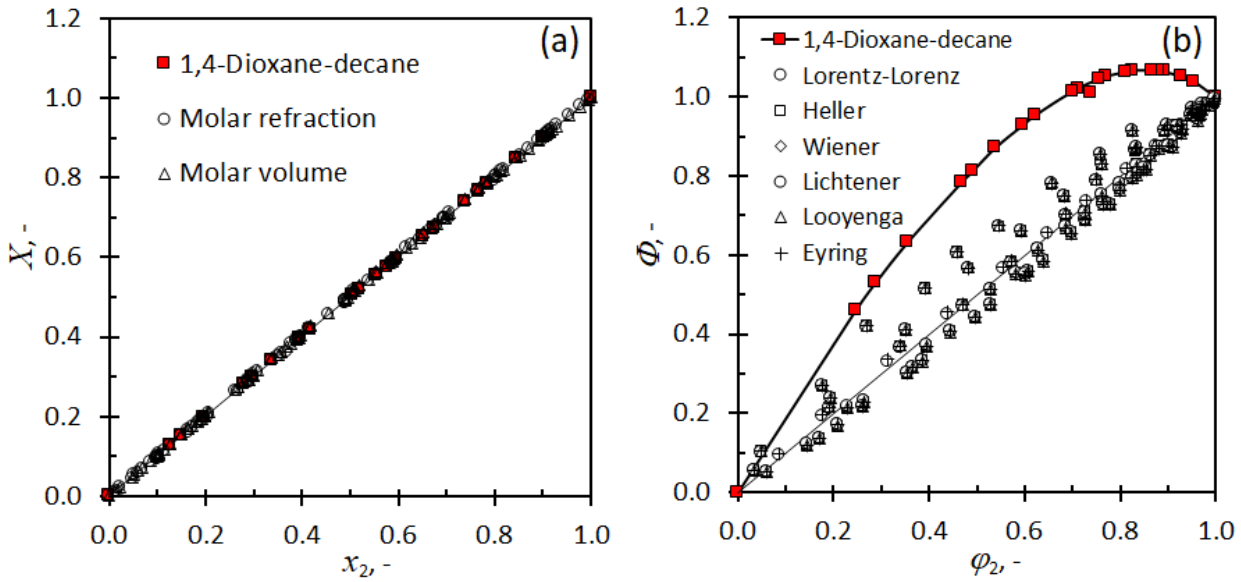

Figure 12: Testing the applicability of the linear mixture models using the binary data of all systems. (a) Equation (94a) applied to the molar volume (Equation (15)) and the Lorentz-Lorenz molar refraction (Equation (18a)). (b) Equation (94b) applied to the mixing rules that assume linear variation with volume fraction.

In order to better understand the reasons for this failure, it is useful to consider actual plots of the refractive index vs. volume fraction. Figure 13 shows representative plots that reveal some of the data trends that were found in the systems studied. In this figure, the data are plotted and shown together with the predictions of the two Lorentz-Lorenz equations. The predictions of the *L-L-R*-mixing rules are indicated by the solid lines. It is clear that they represent the data trends quite well. However, the *L-L-N* mixing rule predictions, represented by dashed lines, fails to adequately describe two out of the three systems considered. While the refractive index data for the chlorobenzene-decane system varies almost linearly with the mole fraction, both the ethanol-octane and the 1,4-dioxane-decane system data deviate from linear behaviour. The *L-L-N* mixture model adequately corrects for the small deviations from linear behaviour for the chlorobenzene-decane system, but it underpredicts the refractive index values of the ethanol-octane system and overpredicts the values for the 1,4 dioxane-decane system.

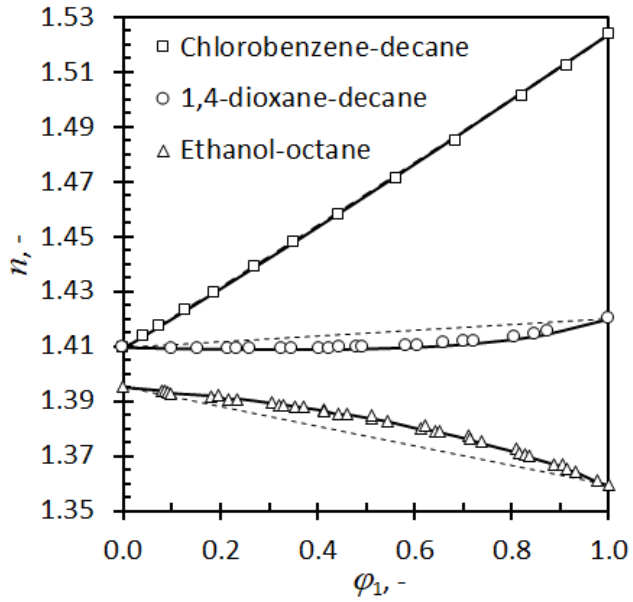

Figure 13: Refractive index data obtained at 25 °C. The solid lines and dashed lines are predictions obtained by applying Equation (18) (the *L*-*L*-*R*-mixing rule) and Equation (22) (the *L*-*L*-*N*-mixing rule) respectively. The two lines for the chlorobenzene-decane system virtually coincide.

Comparison of all the different proposals for defining revised expressions for the N variable show that they all are strictly increasing functions of the refractive index n. In addition, they all assume a linear variation of N with composition expressed in volume fractions. This means that none of these models can represent a minimum in a refractive index vs. composition plot—as is in fact observed in the data of the 1,4-dioxane-decane system. This also explains the values of Φ that exceed unity in Figure 12. They arise from refractive index values in mixtures that are lower than those of both pure compounds.

However, the *L*-*L*-*R* model represents the data for the dioxane-decane system, quite well. Both the molar refraction and the molar volume follow the linear mixing rule in mole fractions. Therefore, Equation (18) can be rearranged as follows:

$$N = \left(R_1 x_1 + R_2 x_2\right)/V \tag{95}$$

Note that, for the mixture, the left-hand side is fully determined by the measured refractive values. Similarly, the right-hand side is fully determined by the density measurements that yield the molar volume of the mixture V. Figure 14 shows plots of these two quantities for binary mixtures of 1,4-dioxane with selected alkanes. The values coincide for all the systems. This implies that variations in the mixture density with temperature are corrected by

concomitant changes in the refractive index in such a way that molar refraction volume retains a linear composition dependence in the mole fractions.

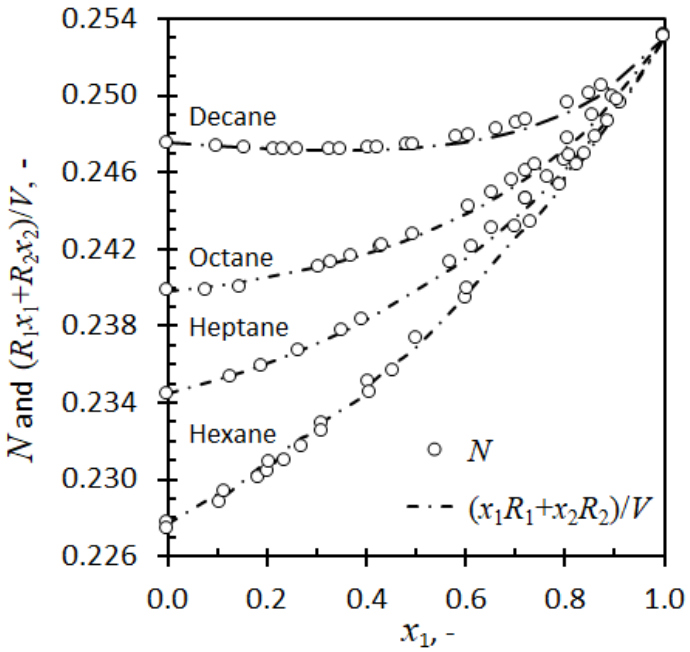

Figure 14: Plots illustrating the link between $N = (n^2-1)/(n^2+2)$, which is the Lorentz-Lorenz expression and the molar volume of binary mixtures of 1,4-dioxane with some alkanes.

4.1.3 Mixture models requiring only refractive index information

So far it has been shown that the *L-L-R* mixture model provides exceptional predictive power. Unfortunately, this model requires density data for the mixture. This is not always convenient to obtain. It is true that the *L-L-N* mixture model works adequately for some binary systems, e.g., the chlorobenzene-decane system (Figure 13). Therefore, it would be useful to determine whether better performance can be achieved for other systems (that are not adequately described by this model) where the refractive index of the mixture suffices for composition determination. In this regard, it is also conspicuous that the proposals for the power index *p* for the power mean-based mixture models, listed in Table 1, vary over such a considerable range, i.e., from zero to two. Such divergent values cannot simultaneously apply to all cases. However, these suggestions were previously supported by experimental results. This suggests that the nature of binary mixtures varies to such an extent that individual systems require unique power indices for proper data representation. Therefore, two approaches for the adjustment of the mixture models were investigated. Firstly, the power-mean mixture models were considered which treat the power index *p* as an adjustable constant. Secondly, the modified

Eykman expression (Piñeiro *et al*, 1999) which allows the parameter *d* to vary, was considered. Least squares regression was used to determine the best data fit for each possibility.

This is shown in Figure 15 as a Φ vs. φ_2 plot. The values of the adjustable parameters and the Φ-φ_2 correlation coefficients (*r*) are listed in Table 8. It is clear that, except for the anisole-dodecane system, better performance is possible with these approaches than is possible with the *L-L-N* mixture model.

Table 8: Φ-φ_2 correlation coefficients and values for the adjustable parameters (*p* and *d*) for the modified Eyckman and volume fraction weighted power mean models

System	Lorentz-Lorenz-N	Power mean		Modified Eykman	
	r	*p*	*r*	*d*	*r*
Acetone-dodecane	0.99953	−4.174	0.99980	−0.682	0.99980
Anisole-dodecane	0.99924	−4.082	0.99891	−0.738	0.99874
Benzene-hexadecane	0.98809	−26.74	0.99921	−1.83	0.99919
Chlorobenzene-decane	0.99990	−0.790	0.99995	0.927	0.99995
Cyclohexanone-dodecane	0.99577	−34.09	0.99963	−1.82	0.99961
Ethanol-octane	0.99823	−16.82	0.99929	−1.50	0.99928

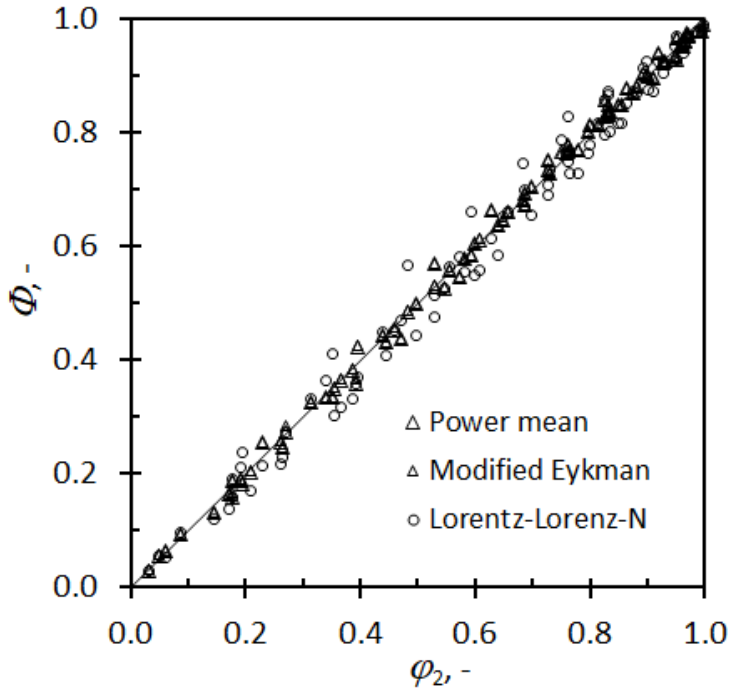

Figure 15: Performance of the Modified Eykman and volume fraction weighted power mean model for correlating the data for the binary systems listed in Table 8.

4.2 DEET phase envelopes

The Flory-Huggins theory is unable to represent the phase envelopes in the vicinity of the critical temperature. However, Diekmann *et al* (2020) indicated that this theory does show the correct trends for the variation of the critical temperature with the molar mass of alkanes.

Figure 3 previously showed that the refractive index of the alkanes was perfectly linear with temperature. This was also the case for DEET. If no phase separation occurs, one would expect that a mixture of DEET and these alkanes would also have a linear refractive index trend with slopes intermediate in magnitude to those of the two pure components. For DEET and octacosane, Figure 16(a) illustrates that starting at 90 °C, this was indeed the case. Equation (24) was applied to transform the *n*-temperature data to the temperature-composition data in Figure 16(b). Thus, the linear sections at high temperature appear as vertical lines in Figure 16(b) because they correspond to homogenous mixtures (fixed compositions).

However, below a characteristic temperature, each refractive index trajectory shows a sudden deviation from linearity. This is indicative of a change in composition in the liquid being sampled and it is indicative of phase separation.

Several additional temperature scans were used with samples consisting of different starting compositions to establish these phase boundaries. The same type of behaviour was seen for all the DEET-alkane mixtures. These lines divide the plane into three separate regions. The phase present in Region I corresponds to the homogeneous liquid state (e.g., Figure 17). Region II is a two-phase zone as the solution has separated into separate liquid phases (e.g., Figure 18). Region III corresponds to solid-liquid equilibrium (e.g., Figure 19). Here the phase boundary line defines the composition of the liquid in equilibrium with solid alkane crystals.

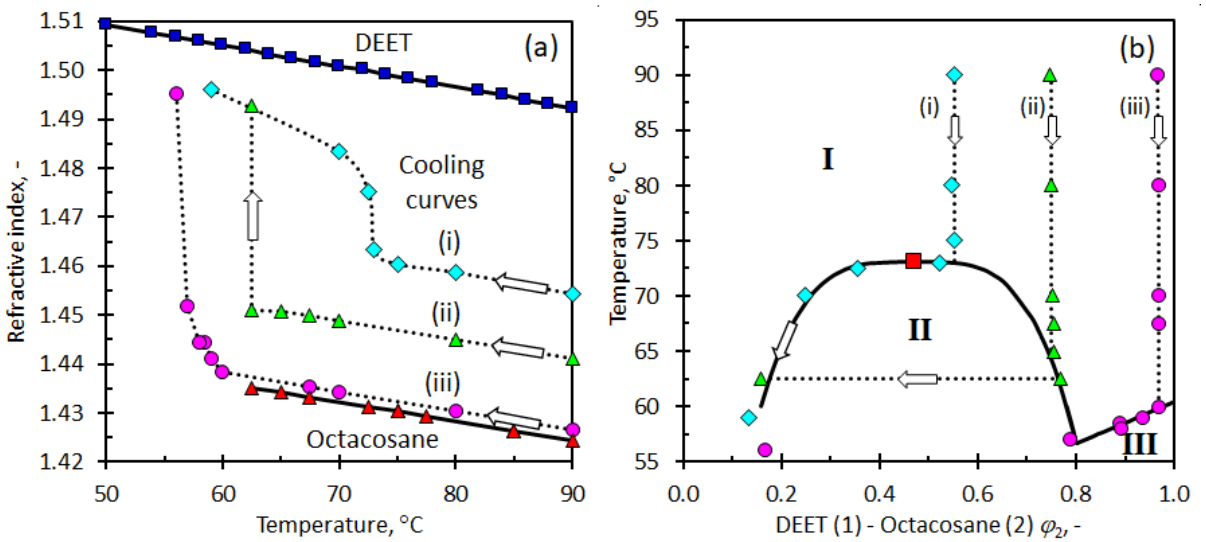

Figure 16: Data for three different mixtures of DEET with octacosane, initially equilibrated as homogeneous solutions at 90 °C. (a) Measured refractive indices as the samples were cooled. Pure DEET and octacosane are indicated as solid black lines at the top and bottom of the plot. (b) Outline of the phase envelopes. The red square shows the critical temperature at the critical volume fraction.

Figure 17: Homogenous dodecane-DEET mixtures in the oven.

Figure 18: Heterogenous dodecane-DEET mixtures after cooling with two liquid layers.

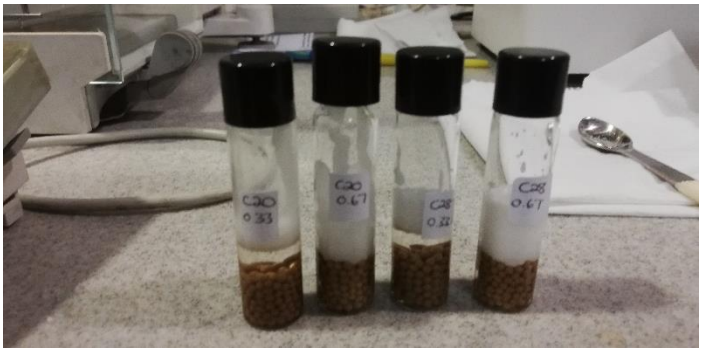

Figure 19: Solid eicosane or octacosane on top of a liquid DEET layer at room temperature.

As mentioned, the cooling trajectories in Region I of Figure 16(b) should correspond to vertical lines as the composition of the mixture remains constant. However, once a phase boundary is traversed, a deviation in this trend is observed for the refractive index. This is caused by a change in the composition of the liquid in contact with- and detected by the sensor. If sufficient time is allowed for equilibration, the measured compositions will in fact trace out the location of the phase boundaries in Figure 16(b). This happened, for example, for the sample (iii) that contained only a small amount of DEET. It traced out the solid-liquid phase boundary in the region where the octacosane crystallised, i.e., it defined the melting point depression curve. The composition locus for sample (i) traced out the left part of the liquid-liquid phase boundary. Sample (ii) showed a sudden jump from the initial composition to one of a much lower octacosane concentration. Both of these effects are due to gravity. It causes the denser phase to accumulate at the bottom of the cell where the measurement window of the instrument is located.

The phase envelopes for the all the DEET-alkane combinations were determined using the procedure described above. The final results are presented in Figure 20.

Estimates for the possible values of the UCST for a DEET-polyethylene mixture were then obtained. The results are presented in Table 9 and in Figure 21. Diekmann *et al* (2020) assumed a linear variation in T_c, yet both their approach and that of Flory-Huggins provided similar UCST estimates.

Table 9: Projected T_c (UCST) values for the DEET-polyethylene system.

Approach/ Equation	Coefficients		Correlation	UCST	95 % confidence interval
Flory-Huggins: $\chi_c = A + B/T_c$	A	B	r	°C	°C
	−1.8958	1.1131	0.9902	183.4	148.0–217.1
Diekmann *et al* (2020): $T_c = a + bT_{crit}$	a	b	r	°C	°C
	117.1	0.2762	0.9946	180.1	162.1–198.2

Figure 21(a) shows that the values for octane to tetradecane lie on a straight line (with B fit by setting $1000/T_c$ as the x-value for the straight line). The correlation coefficient is equal to 0.9902. The limiting value for the UCST for polyethylene is determined from its χ_c value as 183.4 °C. Figure 21(b) also shows that the values for octane to tetradecane lie on a straight line with a correlation coefficient equal to 0.9946. The limiting value for the UCST for polyethylene is determined from the estimated theoretical T_{crit} value at infinite molar mass as 180.1 °C. Both approaches yielded estimates for the UCST that are well above the melting point range of the polyethylene (ca. 126°C) that was used by Mapossa *et al* (2019) to prepare mosquito-repellent anklets. The implication is that they were correct in assuming that the microporous microstructure resulted from an initial liquid-liquid phase separation.

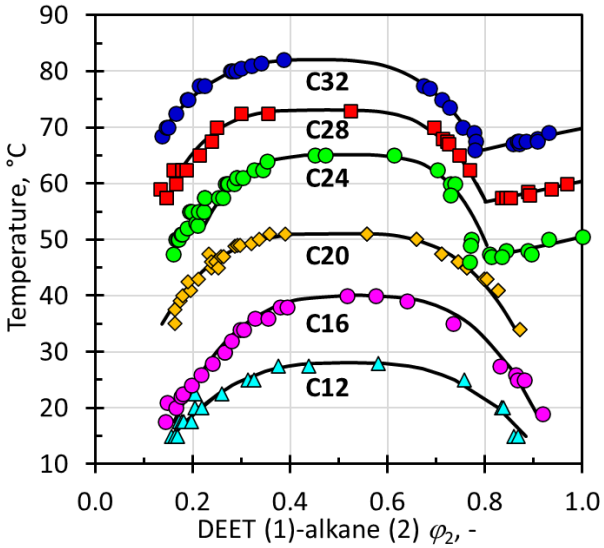

Figure 20: Phase diagram derived from refractive index temperature scans for binary mixtures of DEET with the series of alkanes listed in Table 3. The temperature is plotted against the volume fraction alkane in the mixture.

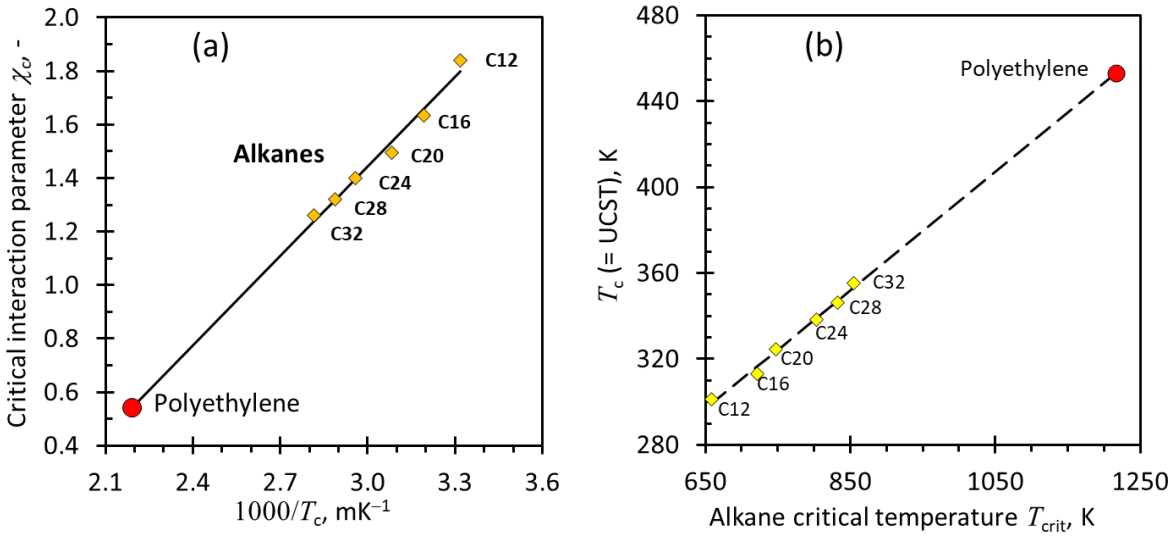

Figure 21: (a) Variation of χ_c *vs.* the UCST (T_c) for mixtures of DEET with a series of alkanes. (b) Variation of the UCST (T_c) with the critical temperature of the alkane (T_{crit}) in the mixture with DEET.

4.3 Padé approximants

The normalised ΔAIC values are shown in Figure 22, separated based on whether the adjustable pure component property (β_i) was based on molar volume or molar mass. The normalised ΔAIC values varied from zero for the $P(1,1)$ Padé reference equation (expected for ideal solutions), to unity for the best performing model variant. Both model D and F performed well considering that they use the most adjustable parameters and allowed them to vary freely. However, model F performed poorly when the regression was limited to the binary data by applying molar

masses. This may be due to overfitting of the binary data because model E, with fewer adjustable coefficients, performed better than model F.

Intermediate values provide relative measures of model performance. When negative values were obtained for a particular model, it indicates that it performed worse than the fully predictive "ideal" solution expression. Often, the value obtained with the binaries was only slightly less than what was achieved with the ternaries. This indicates that the ternary response can reliably be predicted from knowledge of binary data.

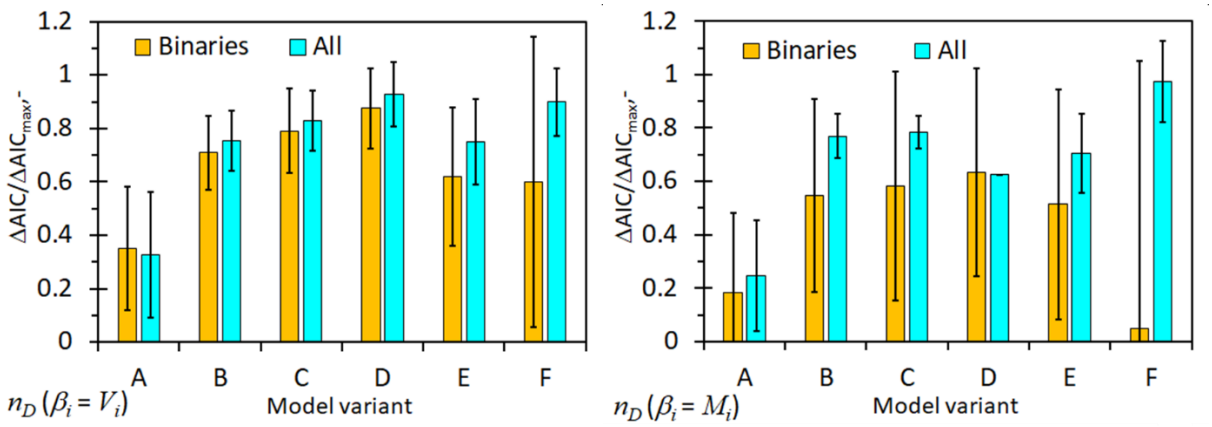

Figure 22: Scaled ΔAIC values for the six model variants averaged over the nine ternary systems (listed in Table 5) for the mixture refractive index.

The ΔAIC values are based on a statistic affected by the sum of the square errors. In contrast, AAD values represent absolute deviations between predictions and actual measurements. Both measures need to be considered to form an accurate view of the model utility. Figure 23 shows that, on average, all model variants performed better than the fully predictive "ideal" solution expressions. The exception is model F where regression of binary data resulted in worse AAD values. Overall, better fits were obtained when all data sets were considered, as opposed to just using the binaries.

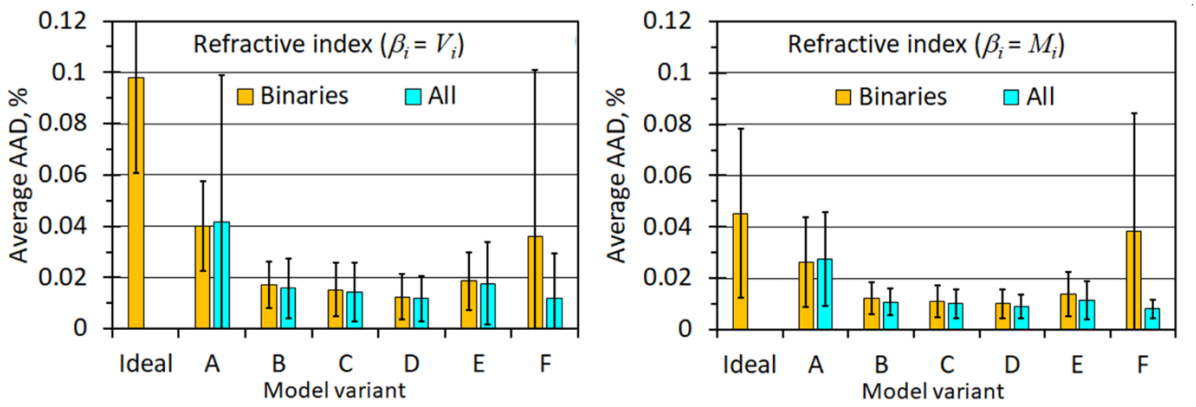

Figure 23: Average absolute deviation (AAD) values achieved with the six model variants for refractive index for the nine ternary systems listed in Table 5.

The goodness of fit can also be visually ascertained. Figure 24 to Figure 32 show the experimental literature refractive index measurements along with the ternary surface plot in OriginLab. The fit was determined by model F and $\beta_i = V_i$. In other words,

$$N = \frac{V_1 x_1 N_1 (x_1 + \kappa_{12} x_2 + \kappa_{13} x_3) + V_2 x_2 N_2 (\kappa_{21} x_1 + x_2 + \kappa_{23} x_3) + V_3 x_3 N_3 (\kappa_{31} x_1 + \kappa_{32} x_2 + x_3)}{V_1 x_1 (x_1 + \lambda_{12} x_2 + \lambda_{13} x_3) + V_2 x_2 (\lambda_{21} x_1 + x_2 + \lambda_{23} x_3) + V_3 x_3 (\lambda_{31} x_1 + \lambda_{32} x_2 + x_3)} \quad (96)$$

This approach also allows measurement errors to be readily seen. Consider the outlier at (0.1, 0.85, 0.05) in Figure 28. This underscores the suitability of Padé expressions to interpolate certain physical property data where measurements may be sparse.

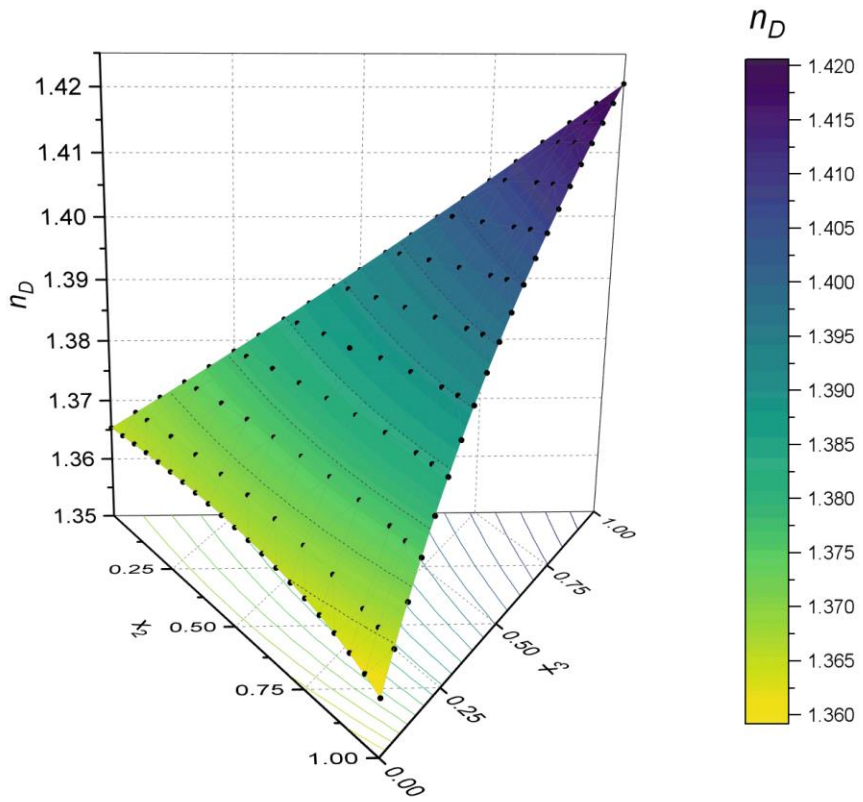

Figure 24: Ternary surface plot of System II at 25 °C with source listed in Table 5.

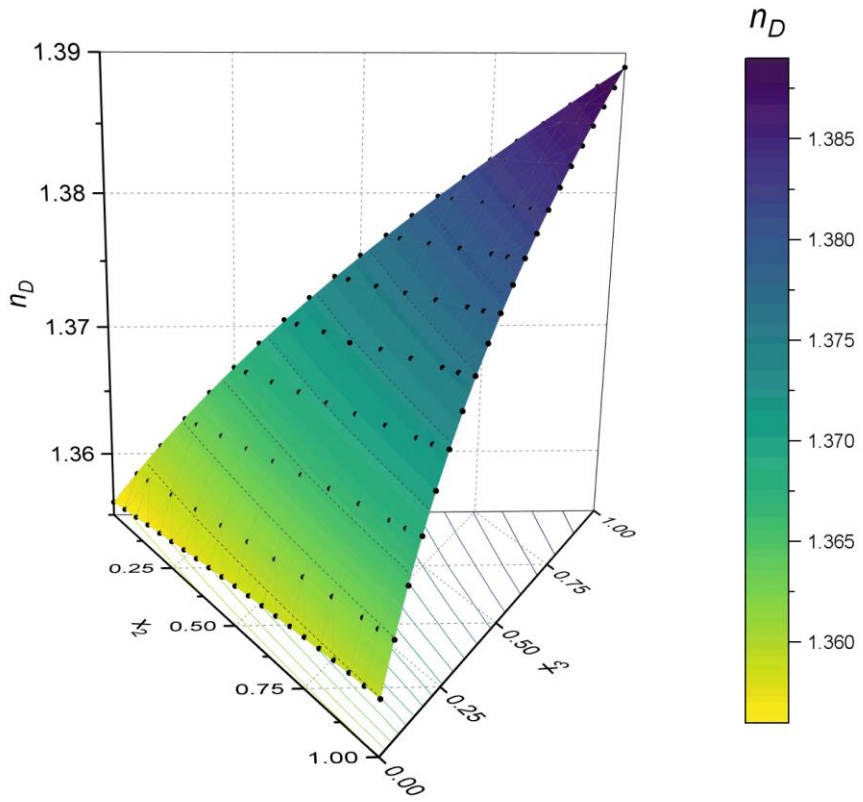

Figure 25: Ternary surface plot of System III at 25 °C with source listed in Table 5.

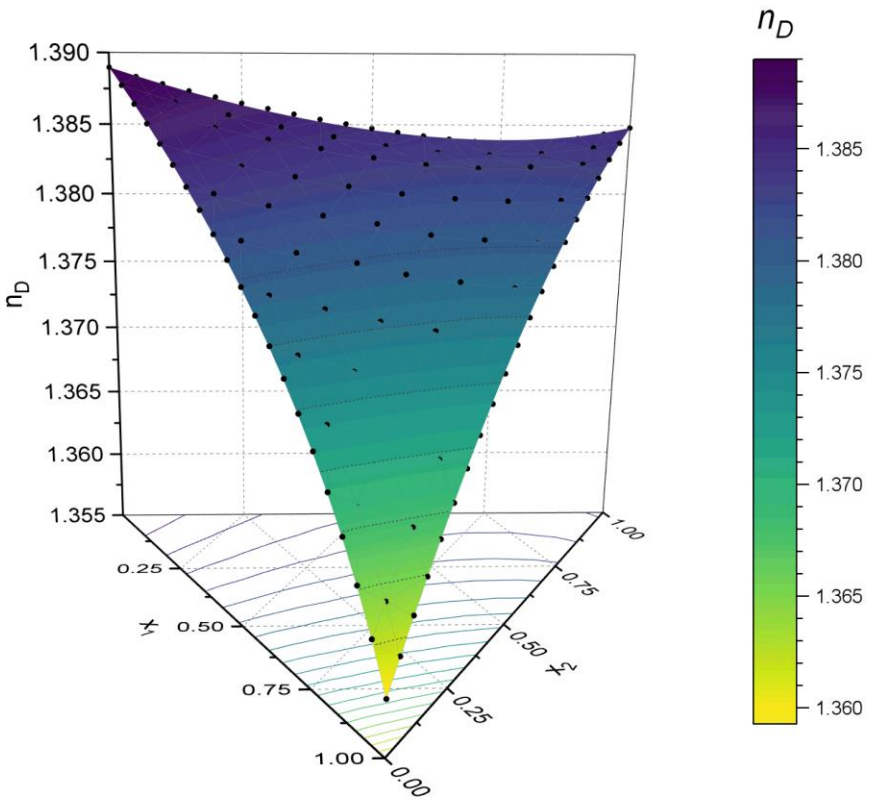

Figure 26: Ternary surface plot of System IV at 25 °C with source listed in Table 5.

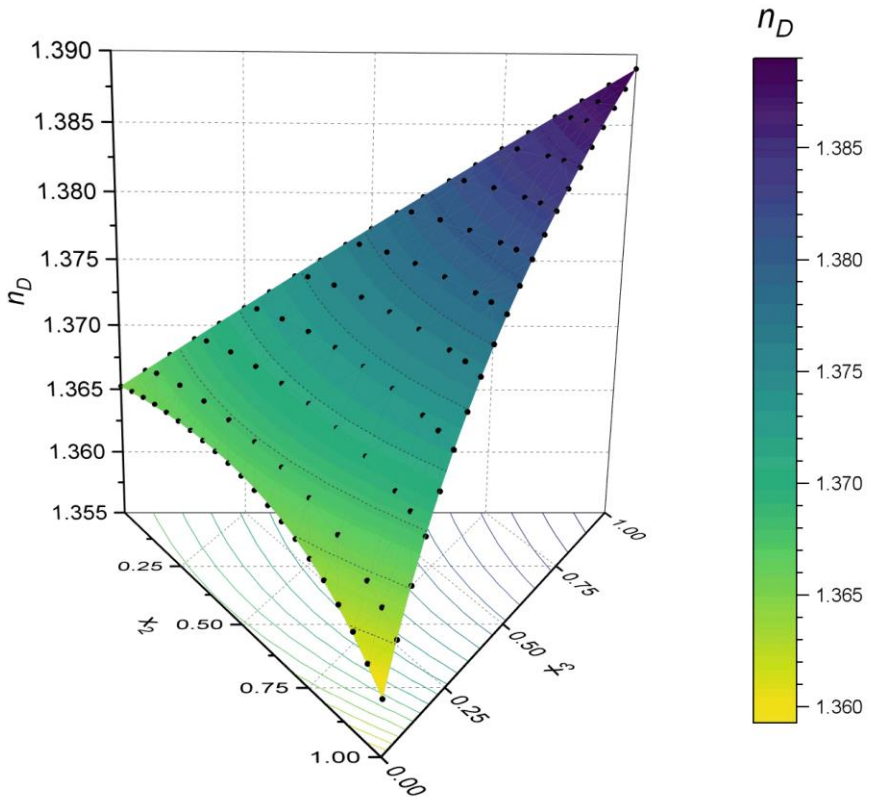

Figure 27: Ternary surface plot of System V at 25 °C with source listed in Table 5.

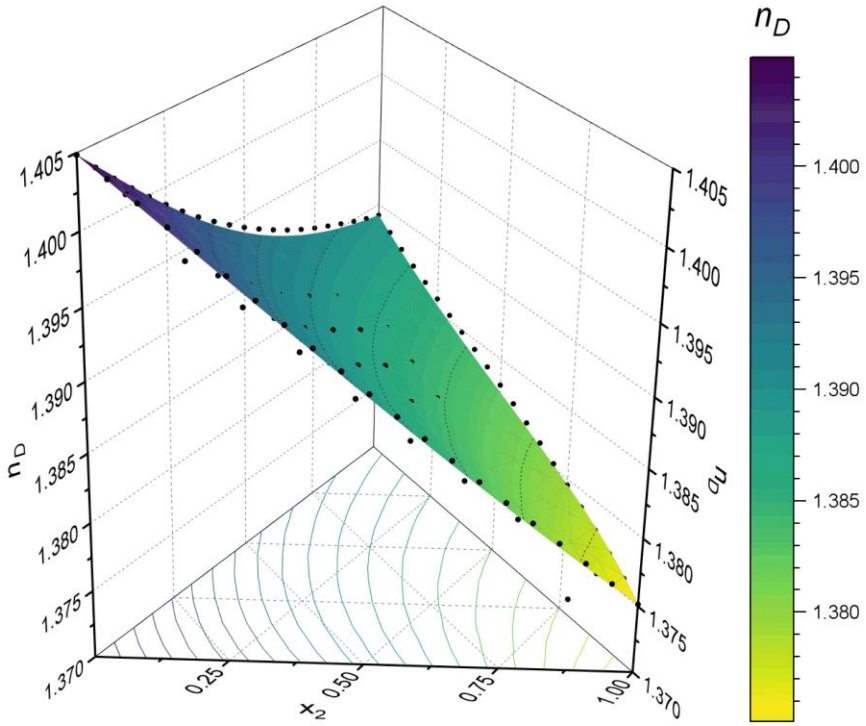

Figure 28: Ternary surface plot of System VI at 25 °C with source listed in Table 5 (note the outlier clearly indicated).

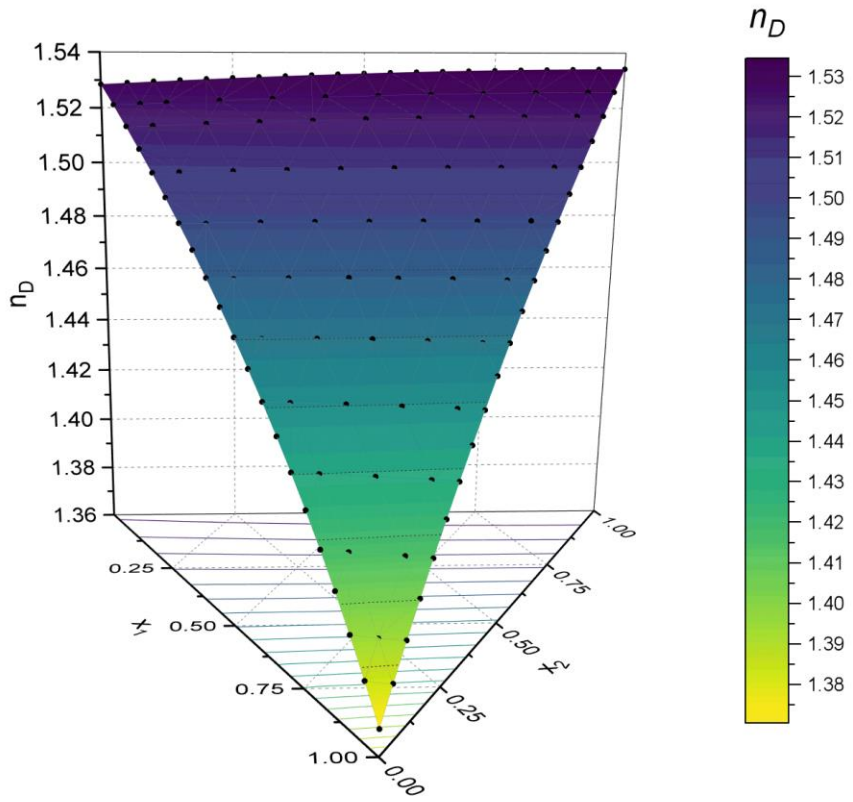

Figure 29: Ternary surface plot of System VII at 35 °C with source listed in Table 5.

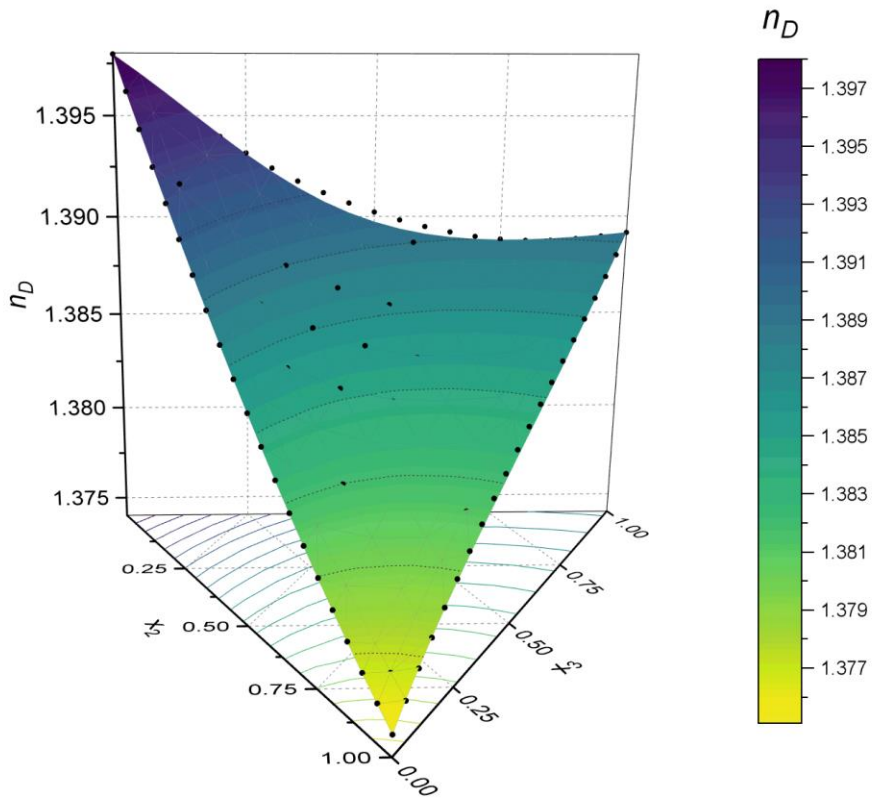

Figure 30: Ternary surface plot of System VIII at 25 °C with source listed in Table 5.

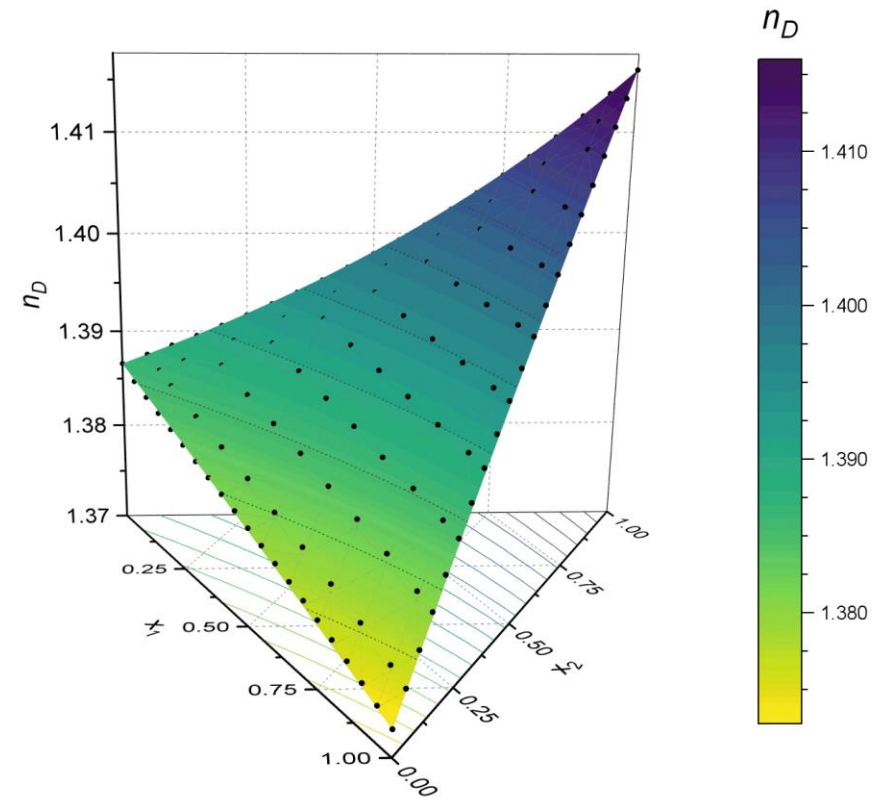

Figure 31: Ternary surface plot of System IX at 30°C with source listed in Table 5.

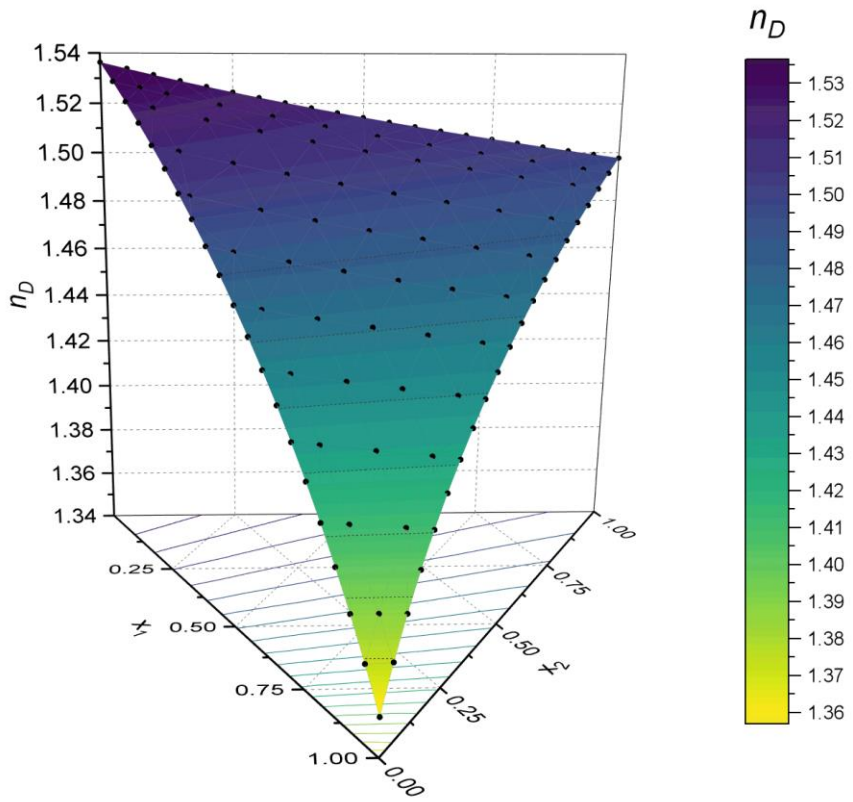

Figure 32: Ternary surface plot of System X at 30°C with source listed in Table 5.

5 Conclusions and recommendations

The importance of determining composition from refractive index and density measurements was emphasised. Among other applications, this can be used in polymer-solvent composite analysis and process simulation.

Several binary mixing rules were reviewed, and it was shown that they can be cast in forms which are linear in mole fraction (dubbed the *L-L-R* mixing rule) or volume fraction. (dubbed the *L-L-N* mixing rule). For pure *n*-alkanes it was shown that the refractive index increases with increased molar mass. Furthermore, the "one-third rule" was shown to apply as well. Binary mixtures of alkanes with aromatic and/or polar compounds showed that the molar refraction is a scaled version of the molar volume, but conveniently temperature invariant. The insight is that the temperature-based changes to the density and refractive index concurrently cancel each other out. Mole fractions are the recommended composition descriptor, as volume fractions are ill-defined. Thus, the *L-L-R* mixing rule is preferred; however, this requires measurements of the mixture density. When these values are not available, the power mean and modified Eyckman relations can be used in terms of volume fraction by regressing their adjustable constants. These were shown to be Padé-type expressions.

The refractive indices of polymer-solvent composites can be used to establish the phase equilibrium boundaries when these mixtures exhibit liquid-liquid or solid-liquid phase separation. Mixtures of DEET and *n*-alkanes were used as analogues for microporous polyethylene products that are used as mosquito repellents. Since the pure components exhibit a linear relationship between refractive index and temperature, the homogenous mixtures at high temperatures also exhibit linear slopes which are intermediate in magnitude to those of the two pure components. However, below a characteristic temperature, a jump discontinuity is observed which corresponds to the onset of liquid-liquid phase separation. A third region is also observed which corresponds to solid-liquid equilibrium. This data was then used to extrapolate towards a straight-chain alkane of infinite molar mass (i.e., polyethylene). The critical Flory-Huggins interaction parameter was then used to estimate the upper critical solution temperature of the DEET-polyethylene system to be ca. 181 °C. This proved to be well above the melting temperature of polyethylene, indicating that liquid-liquid phase separation is the mechanism whereby the microporous structure was formed.

Finally, the idea of extending binary refractive index measurements to ternary systems through Padé approximants was explored. A Padé approximant is a rational function analogue of the Taylor polynomials and can be readily extended to multicomponent mixtures. A parameter-sparse nested polynomial formulation was developed in which the temperature dependence is contained in a pure component property, either molar volume or molar mass. Six different sets of parameter constraint were compared on nine systems of ternary literature data. The difference in Akaike information criterion and average absolute deviation were applied for each case and normalised in comparison to the "ideal" system. Firstly, it was determined that models with the most freely varying adjustable parameters performed the best. Secondly, better fits were obtained when all data sets were considered, as opposed to just using the binaries. Thirdly, the molar volume proved to be a better pure component property than molar mass for scaling to the mixture property. This approach visually highlights outliers as a result of measurement errors.

6 References

Acosta, J, Arce, A, Rodil, E, and Soto, A (2001), "Densities, speeds of sound, refractive Indices, and the corresponding changes of mixing at 25 °C and atmospheric pressure for systems composed by ethyl acetate, hexane, and acetone" *Journal of Chemical & Engineering Data*, 46(5), 1176-1180, https://doi.org/10.1021/je0100490.

Aizpiri, AG, Monroy, F, del Campo, C, Rubio, RG, and Díaz Peña, M (1992), "Range of simple scaling and critical amplitudes near a LCST. The 2-butoxyethanol + water system" *Chemical Physics*, 165(1), 31-39, https://doi.org/10.1016/0301-0104(92)80040-3.

Akaike, H (1983), "Information measures and model selection" *Bulletin of the International Statistical Institute*, 50, 277-290.

Akhtar, MU, and Focke, WW (2015), "Trapping citronellal in a microporous polyethylene matrix" *Thermochimica Acta*, 613, 61-65, https://doi.org/10.1016/j.tca.2015.06.003.

Al-Jimaz, AS, Al-Kandary, JA, Abdul-latif, A-HM, and Al-Zanki, AM (2005), "Physical properties of {anisole + *n*-alkanes} at temperatures between (293.15 and 303.15) K" *The Journal of Chemical Thermodynamics*, 37(7), 631-642, https://doi.org/10.1016/j.jct.2004.09.021.

Andrianov, I, and Shatrov, A (2021), "Padé approximants, their properties, and applications to hydrodynamic problems" *Symmetry*, 13(10), https://doi.org/10.3390/sym13101869.

Arago, DFJ, and Biot, JB (1806), "Refractive properties of binary mixtures" *Mémoires de l'Académie (royale) des sciences de l'Institut (imperial) de France*, 7-9.

Aralaguppi, MI, Jadar, CV, and Aminabhavi, TM (1999), "Density, refractive index, viscosity, and speed of sound in binary mixtures of cyclohexanone with hexane, heptane, octane, nonane, decane, dodecane, and 2,2,4-trimethylpentane" *Journal of Chemical & Engineering Data*, 44(3), 435-440, https://doi.org/10.1021/je9802266.

Bashkatov, A, and Genina, E (2003), "Water refractive index in dependence on temperature and wavelength: a simple approximation" *Saratov Fall Meeting 2002 Laser Physics and Photonics, Spectroscopy, and Molecular Modeling III; Coherent Optics of Ordered and Random Media III*, 5068, https://doi.org/10.1117/12.518857.

Bellman, R (1968), *Approximate Methods*, in*: Mathematics in Science and Engineering*, Bellman, R (ed.) Elsevier.

Bernstein, S (1912), "Démonstration du théorème de Weierstrass fondée sur le calcul des probabilités" *Communications of the Kharkov Mathematical Society*, Volume XIII, 1-2.

Blanco, A, Gayol, A, Gómez, D, and Navaza, JM (2013), "Refractive indices, excess molar volumes and isentropic compressibilities of the mixture of ethanol + *n*-hexane + *n*-nonane in function of the temperature" *Physics and Chemistry of Liquids*, 51(2), 233-246, https://doi.org/10.1080/00319104.2012.737792.

Borowski, E, and Borwein, J (2005), *Collins Dictionary of Mathematics*, HarperCollins, Glasgow.

Brocos, P, Piñeiro, Á, Bravo, R, and Amigo, A (2003), "Refractive indices, molar volumes and molar refractions of binary liquid mixtures: Concepts and correlations" *Physical Chemistry Chemical Physics*, 5(3), 550-557, https://doi.org/10.1039/b208765k.

Calvar, N, Gómez, E, González, B, and Domínguez, Á (2009), "Experimental densities, refractive indices, and speeds of sound of 12 binary mixtures containing alkanes and aromatic compounds at T=313.15K" *The Journal of Chemical Thermodynamics*, 41(8), 939-944, https://doi.org/10.1016/j.jct.2009.03.009.

Calvo, E, Brocos, P, Bravo, R, Pintos, M, Amigo, A, Roux, AH, and Roux-Desgranges, G (1998), "Heat capacities, excess enthalpies, and volumes of mixtures containing cyclic ethers. 1. Binary systems 1,4-dioxane + *n*-alkanes" *Journal of Chemical & Engineering Data*, 43(1), 105-111, https://doi.org/10.1021/je9701691.

Casás, LM, Touriño, A, Orge, B, Marino, G, Iglesias, M, and Tojo, J (2002), "Thermophysical properties of acetone or methanol + *n*-alkane (C9 to C12) mixtures" *Journal of Chemical & Engineering Data*, 47(4), 887-893, https://doi.org/10.1021/je0103059.

Castro, AJ (1981), "Methods for making microporous products", *US 4247498 A*, assigned to Axzona Inc, USA.

Caudwell, DR, Trusler, JPM, Vesovic, V, and Wakeham, WA (2004), "The viscosity and density of *n*-dodecane and *n*-octadecane at pressures up to 200 MPa and temperatures up to 473 K" *International Journal of Thermophysics*, 25(5), 1339-1352, https://doi.org/10.1007/s10765-004-5742-0.

Cerdeiriña, CA, Anisimov, MA, and Sengers, JV (2006), "The nature of singular coexistence-curve diameters of liquid–liquid phase equilibria" *Chemical Physics Letters*, 424(4), 414-419, https://doi.org/10.1016/j.cplett.2006.04.044.

Chang, S-C, Yang, Y, and Pei, Q (1999), "Polymer solution light-emitting devices" *Applied Physics Letters*, 74(14), 2081-2083, https://doi.org/10.1063/1.123764.

Chen, H-W, and Tu, C-H (2005), "Densities, viscosities, and refractive indices for binary and ternary mixtures of acetone, ethanol, and 2,2,4-trimethylpentane" *Journal of Chemical & Engineering Data*, 50(4), 1262-1269, https://doi.org/10.1021/je050010l.

Chen, H-W, and Tu, C-H (2006), "Densities, Viscosities, and Refractive Indices for Binary and Ternary Mixtures of Diisopropyl Ether, Ethanol, and 2,2,4-Trimethylpentane" *Journal of Chemical & Engineering Data*, 51(1), 261-267, https://doi.org/10.1021/je050367p.

Chen, K-D, Lin, Y-F, and Tu, C-H (2012), "Densities, Viscosities, Refractive Indexes, and Surface Tensions for Mixtures of Ethanol, Benzyl Acetate, and Benzyl Alcohol" *Journal of Chemical & Engineering Data*, 57(4), 1118-1127, https://doi.org/10.1021/je201009c.

Chihara, TS (1978), *An Introduction to Orthogonal Polynomials*, Dover Publishers, Inc, New York.

Dale, TP, and Gladstone, JH (1858), "XXXVI. On the influence of temperature on the refraction of light" *Philosophical Transactions of the Royal Society of London*, 148, 887-894, https://doi.org/10.1098/rstl.1858.0036.

Damay, P, and Leclercq, F (1991), "Asymmetry of the coexistence curve in binary systems. Size effect" *The Journal of Chemical Physics*, 95(1), 590-599, https://doi.org/10.1063/1.461787.

Danner, RP, and High, MS (1993), *Handbook of Polymer Solution Thermodynamics*, John Wiley & Sons, Inc., Hoboken, NJ, USA.

Diaz Peña, M, and Nuñez Delgado, J (1975), "Excess volumes at 323.15 K of binary mixtures of benzene with n-alkanes" *The Journal of Chemical Thermodynamics*, 7(2), 201-204, https://doi.org/10.1016/0021-9614(75)90269-4.

Diekmann, S, Dederer, E, Charmeteau, S, Wagenfeld, S, Kiefer, J, Schröer, W, and Rathke, B (2020), "Revisiting the liquid–liquid phase behavior of *n*-alkanes and ethanol" *The Journal of Physical Chemistry B*, 124(1), 156-172, https://doi.org/10.1021/acs.jpcb.9b07214.

Domb, C (1996), *The Critical Point: A Historical Introduction To The Modern Theory Of Critical Phenomena*, Taylor & Francis, London.

Draper, NR, and Pukelsheim, F (1998), "Mixture models based on homogeneous polynomials" *Journal of Statistical Planning and Inference*, 71(1), 303-311, https://doi.org/10.1016/S0378-3758(98)00012-3.

Duren, P (2012), *Invitation to Classical Analysis*, American Mathematical Society, Rhode Island.

Dutour, S, Jean-Luc Daridon, J-L, and Lagourette, B (2001), "Speed of sound, density, and compressibilities of liquid eicosane and docosane at various temperatures and pressures" *High Temperatures High Pressures*, 33, 371-378, https://doi.org/10.1068/htjr007.

Dymond, JH, and Young, KJ (1981), "Transport properties of nonelectrolyte liquid mixtures—V. Viscosity coefficients for binary mixtures of benzene plus alkanes at saturation pressure from 283 to 393 K" *International Journal of Thermophysics*, 2(3), 237-247, https://doi.org/10.1007/BF00504187.

Dzingai, P, Pretorius, F, and Focke, WW (2024), "Correlating multicomponent surface tension data with Padé approximants. Part I. Surface tension" *Journal of Molecular Liquids*, 396, 124003, https://doi.org/10.1016/j.molliq.2024.124003.

Eykman, JF, and Holleman, AF (1919), "Recherches refractometriques" *De Erven Loosjes*.

Eyring, H, and John, MS (1969), *Significant Liquid Structure*, Wiley Inter Science, New York.

Flory, PJ (1941), "Thermodynamics of high polymer solutions" *The Journal of Chemical Physics*, 9(8), 660-661.

Focke, WW, and Du Plessis, B (2004), "Correlating multicomponent mixture properties with homogeneous rational functions" *Industrial & Engineering Chemistry Research*, 43(26), 8369-8377, https://doi.org/10.1021/ie049415+.

Frobenius, G (1881), "Ueber relationen zwischen den näherungsbrüchen von potenzreihen" *Journal für die Reine und Angewandte Mathematik*, 90, 1-17.

Gallavotti, G (1999), *Statistical Mechanics*, Springer-Verlag, Berlin.

Gallegos, J, and Stokkermans, TJ (2023), "Refractive Index", StatPearls Publishing, https://www.ncbi.nlm.nih.gov/books/NBK592413/ [2024-01-17].

Gayol, A, Iglesias, M, Goenaga, JM, Concha, RG, and Resa, JM (2007), "Temperature influence on solution properties of ethanol + *n*-alkane mixtures" *Journal of Molecular Liquids*, 135(1), 105-114, https://doi.org/10.1016/j.molliq.2006.11.012.

Gayol, A, Touriño, A, and Iglesias, M (2010), "Temperature dependence of the derived properties of mixtures containing chlorobenzene and aliphatic linear alkanes (C6–C12)" *Physics and Chemistry of Liquids*, 48(5), 661-681, https://doi.org/10.1080/00319104.2010.481764.

González, B, González, EJ, Domínguez, I, and Domínguez, A (2010), "Excess properties of binary mixtures hexane, heptane, octane and nonane with benzene, toluene and ethylbenzene at T = 283.15 and 298.15 K" *Physics and Chemistry of Liquids*, 48(4), 514-533, https://doi.org/10.1080/00319100903161499.

Grosberg, A, Khokhlov, A, and Halsey, T (1998), "Giant molecules: Here, there, and everywhere" *Physics Today*, 51, 73-74, https://doi.org/10.1063/1.882152.

Heller, W (1945), "The determination of refractive indices of colloidal particles by means of a new mixture rule or from measurements of light scattering" *Physical Review*, 68(1-2), 5-10, https://doi.org/10.1103/PhysRev.68.5.

Heller, W (1965), "Remarks on refractive index mixture rules" *The Journal of Physical Chemistry*, 69(4), 1123-1129, https://doi.org/10.1021/j100888a006.

Huang, T-T, Yeh, C-T, and Tu, C-H (2008), "Densities, viscosities, refractive indices, and surface tensions for the ternary mixtures of 2-propanol + benzyl alcohol + 2-phenylethanol at T = 308.15 K" *Journal of Chemical & Engineering Data*, 53(5), 1203-1207, https://doi.org/10.1021/je7007445.

Huggins, ML (1941), "Solutions of long chain compounds" *The Journal of Chemical Physics*, 9(5), 440.

Iglesias-Otero, MA, Troncoso, J, Carballo, E, and Romaní, L (2008), "Density and refractive index in mixtures of ionic liquids and organic solvents: Correlations and predictions" *The Journal of Chemical Thermodynamics*, 40(6), 949-956, https://doi.org/10.1016/j.jct.2008.01.023.

IUPAC (2006), *Mixture definition*, in*: IUPAC Compendium of Chemical Terminology*.

Jaywant, SA, Singh, H, and Arif, KM (2022), "Sensors and instruments for Brix measurement: A review" *Sensors*, 22(6), 2290, https://doi.org/10.3390/s22062290.

Jiménez, E, Casas, H, Segade, L, and Franjo, C (2000), "Surface tensions, refractive indexes and excess molar volumes of hexane + 1-alkanol mixtures at 298.15 K" *Journal of Chemical & Engineering Data*, 45(5), 862-866, https://doi.org/10.1021/je000060k.

Kao, Y-C, and Tu, C-H (2011), "Densities, viscosities, refractive indices, and surface tensions for binary and ternary mixtures of 2-propanol, tetrahydropyran, and 2,2,4-trimethylpentane" *The Journal of Chemical Thermodynamics*, 43(2), 216-226, https://doi.org/https://doi.org/10.1016/j.jct.2010.08.019.

Korotchenkov, GS (2011), *Chemical Sensors: Comprehensive Sensors Technologies. Electrochemical and Optical Sensors*, Momentum Press, New York.

Kragh, H (2018), "The Lorenz-Lorentz formula: Origin and early history" *Substantia*, 2(2), 7-18, https://doi.org/10.13128/substantia-56.

Krishnaswamy, RK, and Janzen, J (2005), "Exploiting refractometry to estimate the density of polyethylene: The Lorentz–Lorenz approach re-visited" *Polymer Testing*, 24(6), 762-765, https://doi.org/10.1016/j.polymertesting.2005.03.010.

Ku, H-C, Wang, C-C, and Tu, C-H (2008), "Densities, Viscosities, Refractive Indexes, and Surface Tensions for Binary and Ternary Mixtures of Tetrahydofuran, 2-Propanol, and 2,2,4-Trimethylpentane" *Journal of Chemical & Engineering Data*, 53(2), 566-573, https://doi.org/10.1021/je700626v.

Ku, H-C, Wang, C-C, and Tu, C-H (2009), "Densities, Viscosities, Refractive Indices, and Surface Tensions for the Mixtures of 1,3-Dioxolane + 2-Propanol or + 2,2,4-Trimethylpentane at (288.15, 298.15, and 308.15) K and 1,3-Dioxolane + 2-Propanol + 2,2,4-Trimethylpentane at 298.15 K" *Journal of Chemical & Engineering Data*, 54(1), 131-136, https://doi.org/10.1021/je800664z.

Kumar, A, Krishnamurthy, HR, and Gopal, ESR (1983), "Equilibrium critical phenomena in binary liquid mixtures" *Physics Reports*, 98(2), 57-143, https://doi.org/10.1016/0370-1573(83)90106-0.

Kurtz, SS, and Ward, AL (1936), "The refractivity intercept and the specific refraction equation of Newton. I. Development of the refractivity intercept and comparison with specific refraction equations" *Journal of the Franklin Institute*, 222(5), 563-592, https://doi.org/10.1016/S0016-0032(36)90986-9.

Lal, K, Tripathi, N, and Dubey, GP (2000), "Densities, viscosities, and refractive indices of binary liquid mixtures of hexane, decane, hexadecane, and squalane with benzene at 298.15 K" *Journal of Chemical & Engineering Data*, 45(5), 961-964, https://doi.org/10.1021/je000103x.

Letcher, TM (1984), "Excess volumes of (benzene + a cycloalkane) and of (benzene + an *n*-alkane) at two temperatures" *The Journal of Chemical Thermodynamics*, 16(9), 805-810, https://doi.org/10.1016/0021-9614(84)90027-2.

Lloyd, DR, Kinzer, KE, and Tseng, HS (1990), "Microporous membrane formation via thermally induced phase separation. I. Solid-liquid phase separation" *Journal of Membrane Science*, 52(3), 239-261, https://doi.org/10.1016/S0376-7388(00)85130-3.

Looyenga, H (1965), "Dielectric constants of homogeneous mixture" *Molecular Physics*, 9(6), 501-511, https://doi.org/10.1080/00268976500100671.

Lorentz, GG (1953), *Bernstein Polynomials*, University of Toronto Press, University of Michigan.

Mapossa, AB, Focke, WW, Sitoe, A, and Androsch, R (2020), "Mosquito repellent microporous polyolefin strands" *AIP Conference Proceedings*, 2289 (1), 020062, https://doi.org/10.1063/5.0028432.

Mapossa, AB, Sibanda, MM, Sitoe, A, Focke, WW, Braack, L, Ndonyane, C, Mouatcho, J, Smart, J, Muaimbo, H, Androsch, R, and Loots, MT (2019), "Microporous polyolefin strands as controlled-release devices for mosquito repellents" *Chemical Engineering Journal*, 360, 435-444, https://doi.org/10.1016/j.cej.2018.11.237.

Marino, G, Iglesias, M, Orge, B, Tojo, J, and Piñeiro, MM (2000), "Thermodynamic properties of the system (acetone + methanol + *n*-heptane) at T = 298.15 K" *Journal of Chemical Thermodynamics*, 32, 483-497, https://doi.org/10.1006/jcht.1999.0615.

Marino, G, Piñeiro, MM, Iglesias, M, Orge, B, and Tojo, J (2001), "Temperature dependence of binary mixing properties for acetone, methanol, and linear aliphatic alkanes (C6−C8)" *Journal of Chemical & Engineering Data*, 46(3), 728-734, https://doi.org/10.1021/je000200q.

Martens, M, Hadrich, MJ, Nestler, F, Ouda, M, and Schaadt, A (2020), "Combination of refractometry and densimetry – A promising option for fast raw methanol analysis" *Chemie Ingenieur Technik*, 92(10), 1474-1481, https://doi.org/10.1002/cite.202000058.

McGuire, KS, Laxminarayan, A, and Lloyd, DR (1994), "A simple method of extrapolating the coexistence curve and predicting the melting point depression curve from cloud point data for polymer-diluent systems" *Polymer*, 35(20), 4404-4407, https://doi.org/10.1016/0032-3861(94)90099-X.

Mehra, R (2003), "Application of refractive index mixing rules in binary systems of hexadecane and heptadecane withn-alkanols at different temperatures" *Journal of Chemical Sciences*, 115(2), 147-154, https://doi.org/10.1007/BF02716982.

Nayak, JN, Aralaguppi, MI, and Aminabhavi, TM (2003), "Density, viscosity, refractive index, and speed of sound in the binary mixtures of 1,4-dioxane + ethanediol, + hexane, + tributylamine, or + triethylamine at (298.15, 303.15, and 308.15) K" *Journal of Chemical & Engineering Data*, 48(5), 1152-1156, https://doi.org/10.1021/je030107c.

Orge, B, Iglesias, M, Rodríguez, A, Canosa, JM, and Tojo, J (1997), "Mixing properties of (methanol, ethanol, or 1-propanol) with (*n*-pentane, *n*-hexane, *n*-heptane and n-octane) at 298.15 K" *Fluid Phase Equilibria*, 133(1), 213-227, https://doi.org/10.1016/S0378-3812(97)00031-9.

Orge, B, Marino, G, Iglesias, M, Tojo, J, and Piñeiro, MM (2000), "Thermodynamics of (anisole + benzene, or toluene, or *n*-hexane, or cyclohexane, or 1-butanol, or 1-pentanol) at T = 298.15 K" *Journal of Chemical Thermodynamics*, 32, 617-629, https://doi.org/10.1006/jcht.1999.0625.

Orge, B, Rodríguez, A, Canosa, JM, Marino, G, Iglesias, M, and Tojo, J (1999), "Variation of densities, refractive indices, and speeds of sound with temperature of methanol or ethanol with hexane, heptane, and octane" *Journal of Chemical & Engineering Data*, 44(5), 1041-1047, https://doi.org/10.1021/je9900676.

Oster, G (1948), "The scattering of light and its applications to chemistry" *Chemical Reviews*, 43(2), 319-365, https://doi.org/10.1021/cr60135a005.

Padé, H (1892), "Sur la représentation approchée d'une fonction par des fractions rationnelles" *Annales scientifiques de l'Ecole normale supérieure* 9 (Suppl.), 1-93.

Pandey, JD, Shukla, AK, Soni, NK, Tiwari, KK, and Pandey, N (2007), "Theoretical studies of refractivity of binary and ternary solutions" *Journal of the Indian Chemical Society*, 84(7), 674-678, https://doi.org/10.5281/zenodo.5824249 fatcat:qow3tvsavnd2lkewdcdvs3g7yy.

Pardo, JM, Tovar, CA, González, D, Carballo, E, and Romaní, L (2001), "Thermophysical properties of the binary mixtures diethyl carbonate + (*n*-dodecane or *n*-tetradecane) at several temperatures" *Journal of Chemical & Engineering Data*, 46(2), 212-216, https://doi.org/10.1021/je000197a.

Paredes, MLL, Reis, RA, Silva, AA, Santos, RNG, Ribeiro, MHA, and Ayres, PF (2012), "Thermodynamic modeling and experimental speeds of sound, densities, and refractive indexes of (tetralin + *n*-dodecane)" *The Journal of Chemical Thermodynamics*, 54, 377-384, https://doi.org/10.1016/j.jct.2012.05.023.

Penas, A, Calvo, E, Pintos, M, Amigo, A, and Bravo, R (2000), "Refractive indices and surface tensions of binary mixtures of 1,4-dioxane + *n*-alkanes at 298.15 K" *Journal of Chemical & Engineering Data*, 45(4), 682-685, https://doi.org/10.1021/je000038r.

Piñeiro, Á, Brocos, P, Amigo, A, Pintos, M, and Bravo, R (1999), "Surface tensions and refractive indices of (tetrahydrofuran + *n* -alkanes) at T = 298.15 K" *The Journal of Chemical Thermodynamics*, 31(7), 931-942, https://doi.org/10.1006/jcht.1999.0517.

Prausnitz, JM, Lichtenthaler, RN, and Gómes de Azevedo, E (1999), *Molecular Thermodynamics of Fluid-Phase Equilibria*, Prentice-Hall, New Jersey, USA.

Prescott, P, Dean, AM, Draper, NR, and Lewis, SM (2002), "Mixture experiments: Ill-conditioning and quadratic model specification" *Technometrics*, 44(3), 260-268, https://doi.org/10.1198/004017002188618446.

Pretorius, F, Dzingai, P, du Toit, EL, and Focke, WW (2024), "(Submitted for review) Correlating multicomponent physical property data with Padé approximants: Part II. Projecting pure component behaviour".

Pretorius, F, Focke, WW, Androsch, R, and du Toit, E (2021), "Estimating binary liquid composition from density and refractive index measurements: A comprehensive review of mixing rules" *Journal of Molecular Liquids*, 332, https://doi.org/10.1016/j.molliq.2021.115893.

Queimada, AJ, Marrucho, IM, Coutinho, JAP, and Stenby, EH (2005), "Viscosity and liquid density of asymmetric *n*-alkane mixtures: Measurement and modeling" *International Journal of Thermophysics*, 26(1), 47-61, https://doi.org/10.1007/s10765-005-2352-4.

Radović, IR, Kijevčanin, ML, Gabrijel, MZ, Šerbanović, SP, and Djordjević, BD (2008), "Prediction of excess molar volumes of binary mixtures of organic compounds from refractive indices" *Chemical Papers*, 62(3), 302-312, https://doi.org/10.2478/s11696-008-0027-x.

Reif-Acherman, S (2010), “The history of the rectilinear diameter law” *Química Nova*, 33, 2003-2010, https://doi.org/10.1590/S0100-40422010000900033.

Riazi, MR, Enezi, GA, and Soleimani, S (1999), “Estimation of transport properties of liquids” *Chemical Engineering Communications*, 176(1), 175-193, https://doi.org/10.1080/00986449908912152.

Ridgway, K, and Butler, PA (1967), “Physical properties of the ternary system benzene-cyclohexane-hexane” *Journal of Chemical & Engineering Data*, 12(4), 509-515, https://doi.org/10.1021/je60035a012.

Rodrigues, R (2023), "The refractometer, how It works and role in the food industry", Technology Networks, https://www.technologynetworks.com/applied-sciences/articles/the-refractometer-how-it-works-and-role-in-the-food-industry-369653 [2024-01-05].

Scheffé, H (1958), “Experiments with mixtures” *Journal of the Royal Statistical Society: Series B (Methodological)*, 20(2), 344-360, https://doi.org/10.1111/j.2517-6161.1958.tb00299.x.

Schröer, W, and Vale, VR (2009), “Liquid-liquid phase separation in solutions of ionic liquids: Phase diagrams, corresponding state analysis and comparison with simulations of the primitive model” *Journal of Physics Condensed Matter*, 21(42), https://doi.org/10.1088/0953-8984/21/42/424119.

Seborg, DE, Edgar, TF, Mellichamp, DA, and Doyle, FJ (2011), *Process Dynamics and Control*, *International Student Version*, John Wiley & Sons, United States.

Segade, L, Jiménez de Llano, J, Domínguez-Pérez, M, Cabeza, Ó, Cabanas, M, and Jiménez, E (2003), “Density, surface tension, and refractive index of octane + 1-alkanol mixtures at T = 298.15 K” *Journal of Chemical & Engineering Data*, 48(5), 1251-1255, https://doi.org/10.1021/je034053i.

Shehadeh, A, Evangelou, A, Kechagia, D, Tataridis, P, Chatzilazarou, A, and Shehadeh, F (2020), “Effect of ethanol, glycerol, glucose/fructose and tartaric acid on the refractive index of model aqueous solutions and wine samples” *Food Chemistry*, 329, https://doi.org/10.1016/j.foodchem.2020.127085.

Sibanda, M, Focke, W, Braack, L, Leuteritz, A, Brünig, H, Tran, NHA, Wieczorek, F, and Trümper, W (2018), “Bicomponent fibres for controlled release of volatile mosquito repellents” *Materials Science and Engineering C: Materials for Biological Applications*, 91, 754-761, https://doi.org/10.1016/j.msec.2018.06.016.

Singh, RR, and Pitzer, KS (1989), “Relationships in the approach to criticality in fluids, including systematic differences between vapor-liquid and liquid-liquid systems” *The Journal of Chemical Physics*, 90(10), 5742-5748, https://doi.org/10.1063/1.456382.

Sirbu, F, Dragoescu, D, Shchamialiou, A, and Khasanshin, T (2019), “Densities, speeds of sound, refractive indices, viscosities and their related thermodynamic properties for n-hexadecan + two aromatic hydrocarbons binary mixtures at temperatures from 298.15 K to 318.15 K” *The Journal of Chemical Thermodynamics*, 128, 383-393, https://doi.org/10.1016/j.jct.2018.08.036.

Sitoe, A, Mapossa, AB, Focke, WW, Muiambo, H, Androsch, R, and Wesley-Smith, J (2020), "Development, characterization and modeling of mosquito repellent release from microporous devices" *SPE Polymers*, 1(2), 90-100, https://doi.org/10.1002/pls2.10021.

Sitoe, AJ, Pretorius, F, Focke, WW, Androsch, R, and du Toit, EL (2021), "Solid–liquid–liquid phase envelopes from temperature-scanned refractive index data" *Journal of Polymer Engineering*, 41(7), 517-527, https://doi.org/10.1515/polyeng-2021-0062.

Sungkapreecha, C, Focke, WW, and Androsch, R (2020), "Competition between liquid-liquid de-mixing, crystallization, and glass transition in solutions of PLA of different stereochemistry and DEET" *Chinese Journal of Polymer Science (English Edition)*, 38(2), 174-178, https://doi.org/10.1007/s10118-019-2314-0.

Tasic, AZ, Djordjevic, BD, Grozdanic, DK, and Radojkovic, N (1992), "Use of mixing rules in predicting refractive indexes and specific refractivities for some binary liquid mixtures" *Journal of Chemical & Engineering Data*, 37(3), 310-313, https://doi.org/10.1021/je00007a009.

Teja, AS, and Rice, P (1976), "Densities of benzene-*n*-alkane mixtures" *Journal of Chemical & Engineering Data*, 21(2), 173-175, https://doi.org/10.1021/je60069a010.

Thormählen, I, Straub, J, and Grigull, U (1985), "Refractive index of water and its dependence on wavelength, temperature, and density" *Journal of Physical and Chemical Reference Data*, 14(4), 933-945, https://doi.org/10.1063/1.555743.

Tourino, A, Gayol, A, Hervello, M, Moreno, V, and Iglesias, M (2004), "Changes of refractive indices of the ternary mixtures chlorobenzene + *n*-hexane + (*n*-nonane or *n*-decane) at 298.15 K" *Physics and Chemistry of Liquids*, 42(1), 63-74, https://doi.org/10.1080/00319100310001604858.

Ulbricht, M (2006), "Advanced functional polymer membranes" *Polymer*, 47(7), 2217-2262, https://doi.org/10.1016/j.polymer.2006.01.084.

Vale, VR, Rathke, B, Will, S, and Schröer, W (2010), "Liquid−liquid phase behavior of solutions of 1-dodecyl-3-methylimidazolium bis((trifluoromethyl)sulfonyl)amide (C12mimNTf2) in *n*-alkyl alcohols" *Journal of Chemical & Engineering Data*, 55(10), 4195-4205, https://doi.org/10.1021/je100359x.

Vargas, FM, and Chapman, WG (2010), "Application of the one-third rule in hydrocarbon and crude oil systems" *Fluid Phase Equilibria*, 290(1), 103-108, https://doi.org/10.1016/j.fluid.2009.12.004.

Vuksanović, JM, Bajić, DM, Ivaniš, GR, Živković, EM, Radović, IR, Šerbanović, SP, and Kijevčanin, ML (2014), "Prediction of excess molar volumes of selected binary mixtures from refractive index data" *Journal of the Serbian Chemical Society* 79(6), 707–718, https://doi.org/10.2298/JSC130813127V.

Wang, C-C, Chen, H-W, and Tu, C-H (2005), "Densities, viscosities, and refractive indices for binary and ternary mixtures of ethanol, 2-methylpropan-2-ol, and 2,2,4-trimethylpentane" *Journal of Chemical & Engineering Data*, 50(5), 1687-1693, https://doi.org/10.1021/je0501639.

Warner, DJ (2010), *Refractometers and Industrial Analysis*, in*: Illuminating Instruments*, Morris, P, and Staubermann, K (eds.) Smithsonian Institution Scholarly Press, Washington, D.C.

Waxler, RM, and Cleek, GW (1973), "The effect of temperature and pressure on the refractive index of some oxide glasses" *Journal of Research of the National Bureau of Standards. Section A, Physics and Chemistry*, 77A(6), 755–763, https://doi.org/10.6028/jres.077A.046.

Weierstrass, K (1885), "Über die analytische darstellbarkeit sogenannter willkürlicher functionen einer reellen veränderlichen" *Sitzungsberichte der Königlich Preußischen Akademie der Wissenschaften zu Berlin*, 633-639, 789-805.

Weisstein, EW (2024), "Orthogonal functions", MathWorld—A Wolfram Web Resource, https://mathworld.wolfram.com/OrthogonalPolynomials.html [2024-01-19].

Wiener, O (1910), "Die theorie des mischkörpers für das feld der stationären strömung " *Berichte über die Verhandlungen der Königlich-Sächsischen Gesellschaft der Wissenschaften zu Leipzig, Mathematisch-Physische Klasse*, 62, 256-277.

Wohl, K (1946), "Thermodynamic evaluation of binary and ternary liquid systems" *Transactions of the American Institute of Chemical Engineers*, 42, 215–249.

Wypych, G (2017), *Typical Methods of Quality Control of Plasticizers*, in*: Handbook of Plasticizers*, 3rd ed, Wypych, G (ed.) ChemTec Publishing.

Yaws, CL, and Pike, RW (2009), *Chapter 3 - Density of Liquid—Organic compounds*, in*: Thermophysical Properties of Chemicals and Hydrocarbons*, Yaws, CL (ed.) William Andrew Publishing, Norwich, NY.

Ye, J-D, and Tu, C-H (2005), "Densities, Viscosities, and Refractive Indices for Binary and Ternary Mixtures of Diisopropyl Ether, Ethanol, and Methylcyclohexane" *Journal of Chemical & Engineering Data*, 50(3), 1060-1067, https://doi.org/10.1021/je050031f.

Yeh, C-T, and Tu, C-H (2007), "Densities, Viscosities, Refractive Indexes, and Surface Tensions for Binary Mixtures of 2-Propanol + Benzyl Alcohol, + 2-Phenylethanol and Benzyl Alcohol + 2-Phenylethanol at T = (298.15, 308.15, and 318.15) K" *Journal of Chemical & Engineering Data*, 52(5), 1760-1767, https://doi.org/10.1021/je700140j.

Young, RJ, and Lovell, PA (2011), *Introduction to Polymers*, CRC Press, USA.

Appendix A Derivations

A.1 Composition in binary mixtures from density and refractive index measurements

The derivations for the composition of a component in a binary mixture (Section 2.3.2) are given here.

Case A: Calculating composition from density measurements.

Assume: $$V = V_1 x_1 + V_2 x_2$$

$$\frac{M_1 x_1 + M_2 x_2}{\rho} = \frac{M_1 x_1}{\rho_1} + \frac{M_2 x_2}{\rho_2}$$

$$M_1 x_1 \left(\frac{1}{\rho} - \frac{1}{\rho_1}\right) + M_2 x_2 \left(\frac{1}{\rho} - \frac{1}{\rho_2}\right) = 0$$

$$M_1 x_1 \left(\frac{1}{\rho} - \frac{1}{\rho_1}\right) + M_2 (1 - x_1) \left(\frac{1}{\rho} - \frac{1}{\rho_2}\right) = 0$$

$$x_1 \left[M_2 \left(\frac{1}{\rho} - \frac{1}{\rho_2}\right) - M_1 \left(\frac{1}{\rho} - \frac{1}{\rho_1}\right) \right] = M_2 \left(\frac{1}{\rho} - \frac{1}{\rho_2}\right)$$

$$x_1 \left[M_2 \left(\frac{\rho_2 - \rho}{\rho\rho_2}\right) - M_1 \left(\frac{\rho_1 - \rho}{\rho\rho_1}\right) \right] = M_2 \left(\frac{\rho_2 - \rho}{\rho\rho_2}\right)$$

$$x_1 \left[\rho_1 M_2 (\rho_2 - \rho) - \rho_2 M_1 (\rho_1 - \rho) \right] = \rho_1 M_2 (\rho_2 - \rho)$$

$$\frac{1}{x_1} = 1 - \frac{\rho_2 M_1 (\rho_1 - \rho)}{\rho_1 M_2 (\rho_2 - \rho)}$$

Case B: Calculating composition from both density and refractive index measurements.

Assume: $$VN = x_1 V_1 N_1 + x_2 V_2 N_2$$

$$\frac{x_1 M_1 N + x_2 M_2 N}{\rho} = \frac{x_1 M_1 N_1}{\rho_1} + \frac{x_2 M_2 N_2}{\rho_2}$$

$$x_1 \rho_1 \rho_2 M_1 N + x_2 \rho_1 \rho_2 M_2 N = x_1 \rho \rho_2 M_1 N_1 + x_2 \rho \rho_1 M_2 N_2$$

$$x_1 \left[\rho \rho_1 M_2 N_2 - \rho_1 \rho_2 M_2 N + \rho_1 \rho_2 M_1 N - \rho \rho_2 M_1 N_1 \right] = \rho \rho_1 M_2 N_2 - \rho_1 \rho_2 M_2 N$$

$$\frac{1}{x_1} = 1 - \frac{\rho_2 M_1 \left(\rho N_1 - \rho_1 N\right)}{\rho_1 M_2 \left(\rho N_2 - \rho_2 N\right)}$$

Case C: Calculating composition from both density and refractive index measurements when the individual molar refractions are temperature invariant.

Assume:
$$VN = x_1 R_1 + x_2 R_2 = \frac{M_1 x_1 + M_2 x_2}{\rho} N$$

$$x_1 \rho R_1 + x_2 \rho R_2 = N M_1 x_1 + N M_2 x_2$$

$$x_1 \rho R_1 + \left(1 - x_1\right) \rho R_2 = N M_1 x_1 + N M_2 \left(1 - x_1\right)$$

$$x_1 \rho \left(R_1 - R_2\right) + \rho R_2 = x_1 N \left(M_1 - M_2\right) + N M_2$$

$$x_1 [\rho (R_1 - R_2) - N (M_1 - M_2)] = N M_2 - \rho R_2$$

$$x_1 \left[N M_2 - \rho R_2 - \left(N M_1 - \rho R_1 \right) \right] = N M_2 - \rho R_2$$

$$\frac{1}{x_1} = \frac{N M_2 - \rho R_2 - \left(N M_1 - \rho R_1 \right)}{N M_2 - \rho R_2}$$

$$\frac{1}{x_1} = 1 - \frac{N M_1 - \rho R_1}{N M_2 - \rho R_2}$$

Case D: Calculating composition from refractive index measurements of the mixture and pure components using the Lorentz-Lorenz *N*-mixing rule when the mixture density is unavailable.

Assume: Both *V* and *R* follow the linear blending rule

$$VN = x_1 V_1 N_1 + x_2 V_2 N_2$$

$$\varphi_1 = \frac{V_1 x_1}{V_1 x_1 + V_2 x_2} \quad \text{and} \quad \varphi_2 = 1 - \varphi_1 = \frac{V_2 x_2}{V_1 x_1 + V_2 x_2}$$

Take the ratio

$$\frac{\varphi_1}{1 - \varphi_1} = \frac{V_1 x_1}{V_2 (1 - x_1)}$$

$$\varphi_1 V_2 \left(1 - x_1\right) = \left(1 - \varphi_1\right) V_1 x_1$$

$$\left(1 - \varphi_1\right) V_1 x_1 + \varphi_1 V_2 x_1 = x_1 \left[\left(1 - \varphi_1\right) V_1 + \varphi_1 V_2 \right] = \varphi_1 V_2$$

$$x_1 = \frac{\varphi_1 V_2}{\varphi_1 V_2 + \varphi_2 V_1}$$

$$x_1 = \frac{\varphi_1 V_2}{\varphi_1 V_2 + \varphi_2 V_1} = \frac{\varphi_1 \dfrac{R_2}{N_2}}{\varphi_1 \dfrac{R_2}{N_2} + \varphi_2 \dfrac{R_1}{N_1}} = \frac{\varphi_1 N_1 R_2}{\varphi_1 N_1 R_2 + \varphi_2 N_2 R_1}$$

$$x_1 = \frac{N_1 R_2 \dfrac{\left(N - N_2\right)}{\left(N_1 - N_2\right)}}{N_1 R_2 \dfrac{\left(N - N_2\right)}{\left(N_1 - N_2\right)} + N_2 R_1 \dfrac{\left(N - N_1\right)}{\left(N_2 - N_1\right)}}$$

$$x_1 = \frac{N_1 R_2 \left(N - N_2\right)}{N_1 R_2 \left(N - N_2\right) - N_2 R_1 \left(N - N_1\right)}$$

$$\frac{1}{x_1} = 1 - \frac{N_2 R_1 \left(N - N_1\right)}{N_1 R_2 \left(N - N_2\right)}$$

A.2 Extension of two binary data sets to the other in a ternary system

It is shown that if data for only two of the three binaries of a ternary system are available, this suffices to fit all the parameters of the *P*(1,1) Padé model. The model for the ternary system is:

$$p = \frac{\beta_1 x_1 p_1 + \beta_2 x_2 p_2 + \beta_3 x_3 p_3}{\beta_1 x_1 + \beta_2 x_2 + \beta_3 x_3}$$

Assume that binary data is available for mixtures of component (1) + component (2) and for mixtures of component (1) + component (3). No experimental data is available for the remaining binary, i.e. for mixtures of component (2) + component (3). This means that component (1) is common to the two binaries for which data are available. Due to the rational nature of this expression, the parameters are not uniquely defined. Multiplying each of them by an arbitrary constant does not change the predictions. One way to enforce uniqueness is accomplished by dividing throughout with β_1. The full model applicable to the ternary system now reads:

$$p = \frac{x_1 p_1 + \left(\beta_2 / \beta_1\right) x_2 p_2 + \left(\beta_3 / \beta_1\right) x_3 p_3}{x_1 + \left(\beta_2 / \beta_1\right) x_2 + \left(\beta_3 / \beta_1\right) x_3}$$

The model for binary component (1) + component (2) is:

$$p = \frac{x_1 p_1 + (\beta_2/\beta_1) x_2}{x_1 + (\beta_2/\beta_1) x_2}$$

The value of β_2/β_1 is found by regressing the available binary data. Similarly, the model for mixtures of component (1) + component (3) is given by:

$$p = \frac{x_1 p_1 + (\beta_3/\beta_1) x_3 p_3}{x_1 + (\beta_3/\beta_1) x_3}$$

The value of β_3/β_1 is found by regressing the available binary data for this system. Clearly, when these two parameters are known, the ternary behaviour can be predicted. This is also true for the binary component (2) + component (3). The model for this binary is:

$$p = \frac{(\beta_2/\beta_1) x_2 p_2 + (\beta_3/\beta_1) x_3 p_3}{(\beta_2/\beta_1) x_2 + (\beta_3/\beta_1) x_3}$$

In other words, only one value (x_2) is unknown, since $x_3 = 1 - x_2$. Multiplying top and bottom with β_1/β_2 yields:

$$p = \frac{x_2 p_2 + (\beta_3/\beta_2) x_3 p_3}{x_2 + (\beta_3/\beta_2) x_3}$$

Therefore, β_3/β_2 can be predicted from less experimental data than other models.